PERFORMING RING OPENING METATHESIS POLYMERIZATION (ROMP) REACTIONS AND POST-POLYMERIZATION MODIFICATIONS UNDER FLOW CONDITIONS

_____

A Thesis

Presented to

The Faculty of the Department of Chemistry

Sam Houston State University

_____

In Partial Fulfillment

of the Requirements for the Degree of

Master of Science

_____

by

Selesha I. Subnaik

May, 2020

PERFORMING RING OPENING METATHESIS POLYMERIZATION (ROMP) REACTIONS AND POST-POLYMERIZATION MODIFICATIONS UNDER FLOW CONDITIONS

by

Selesha I. Subnaik

_____

APPROVED:

Christopher E. Hobbs, PhD
Committee Director

Dustin E. Gross, PhD
Committee Member

Christopher M. Zall, PhD
Committee Member

John Pascarella, PhD
Dean, College of Science and Engineering Technology

DEDICATION

To my family and friends for the unconditional love and support.

ABSTRACT

Subnaik, Selesha I., *Performing Ring Opening Metathesis Polymerization (ROMP) Reactions and Post-Polymerization Modifications Under Flow Conditions*. Master of Science (Chemistry), May, 2020, Sam Houston State University, Huntsville, Texas.

Ring opening metathesis polymerization (ROMP) reactions of norbornene derived monomers and Grubbs 3rd Generation catalyst were run under continuous flow conditions. Typically, ROMP reactions are performed using "batch" reaction conditions that involve the use of round-bottomed flasks and mechanical stirrers to allow for mixing. Further, these experiments are typically carried out under inert atmospheres to achieve oxygen exclusion and prevent catalyst death, which can affect the expected monomer to initiator ([M]:[I]) ratio of the polymerization reaction. However, under continuous flow conditions, the ROMP reactions in this study were performed under air atmosphere using a simple bench-top setup with syringe pumps, segments of reaction tubing, connectors and syringes that allowed for betting mixing, and excessive reaction times which can lead to less controlled polymerization reactions. Nuclear magnetic resonance (NMR) analysis provided percent conversion of monomer to polymer, and gel permeation chromatography (GPC) analysis provided number-average molecular weights (M_n) and polydispersity index (PDI, $Đ$) values. Homopolymerization reactions were performed with residence times (t_R) of 22.5 s and 7.5 s. $Đ$ values ranged from 1.14-1.33 and 1.07-1.18 for t_R =22.5 s and t_R=7.5s, respectively, for most norbornene derived monomers studied. Monocyclic monomers such as cyclopentene, cyclooctene and cyclooctadiene were not able to be successfully analyzed post polymerization under flow conditions to give an indication of control over the reactions. Block copolymers consisting of a block of norbornene followed by a block of *exo*-functionalized norbornene were synthesized

using a t_R of 22.5 s. Percent conversions were >95% for all block copolymerization reactions. Thio-bromo click reactions were performed in flow where an *exo*-α-bromo ester functionalized norbornene monomer was polymerized in flow and subsequently followed in-line with a solution of thiol and triethylamine for a "click" reaction to occur. Both the polymerization and the thio-bromo click reaction percent conversions were >95% as determined by ^{1}H NMR.

KEY WORDS: Continuous flow, Ring opening metathesis polymerization (ROMP), Norbornene, Homopolymerization, Block copolymerization, Thio-bromo "click" reaction, Post-polymerization modification

ACKNOWLEDGEMENTS

Thank you to my research advisor Dr. Christopher Hobbs for his guidance and support. During my two years here at Sam Houston State University (SHSU) I have had the privilege of improving my understanding of both organic chemistry and polymer science under his tutelage. His dedication to his research and his students in the lab and classroom has helped to make me a more confident and better chemist.

Thank you to both Dr. Dustin Gross and Dr. Christopher Zall for serving on my committee. Their corrections towards my thesis and support for my defense is much appreciated. Thank you to Dr. Arney for the company, great conversation and help (especially during the weekends I've spent doing research in the chemistry building).

Thank you to the faculty and staff of the SHSU Chemistry department who have supported and facilitated the daunting task of pursuing a master's degree less unnerving with their kind words of support and smiling faces.

To my friends, thank you for welcoming me into your friend groups, you all made the sting of living far from family hurt less. I share with you my favorite quote from Maya Angelou: "I've learned that people will forget what you said, people will forget what you did, but people will never forget how you made them feel"—and it's true, I will always remember and appreciate you all being a part of this journey.

Lastly, thank you to my family. Mommy and Daddy, a simple thank you is not enough to express how grateful I am for your unwavering love and support no matter what I choose to do. Thank you for giving me this beautiful life.

TABLE OF CONTENTS

Page

LIST OF TABLES

LIST OF FIGURES

Page

CHAPTER I

Introduction

1.1 Living polymerization

The development and use of controlled ("living") polymerization techniques allows scientists the ability to prepare polymeric materials with astonishing control over structure, morphology, and size.[1] Living polymerizations are defined as polymerization reactions that occur in the absence of termination events; this results in high levels of control over polymer molecular weight. Additionally, these reactions produce polymer chains consisting of active chain ends which can be used to prepare block copolymers. The first truly "living" polymerizations were anionic polymerizations described by Szwarc.[1] It would take another few decades before both controlled ("living") free radical and ring opening metathesis polymerization (CRP and ROMP, respectively) reactions were invented.

In order to impart such fine control over polymerization, typical batch reactions must be carried out to adequately perform these reactions in the absence of air to prevent side reactions or catalyst death, which would negatively impact molecular weight. Polymerizations can require the use of excessive amounts of organic solvent (to keep the synthesized polymer in solution and stirring for a homogenous reaction), generating relatively large amounts of laboratory waste, rendering this a "green" chemistry issue. This problem may be exacerbated in the formation of block copolymers where multiple solvent precipitations may need to be carried out in order to isolate each block. Although it is not always required, batch reactions are typically conducted utilizing a sophisticated apparatus, such as a glove box or Schlenk line.[2]

1.2 Continuous flow polymerization

Continuous flow polymerization reactions offer a range of benefits compared to batch polymerization reactions. The benefits of continuous flow chemistry include: improved heat transfer, enhanced mixing, and superior control over crucial aspects of reactions like temperature and time compared to batch.[3] Through manipulation of the concentration of reactants, the flow rate of reaction, and the ratio of [M]:[I] (or catalyst in some cases), polymers of varying molecular weight can be isolated during the polymerization.[2] Simple scale up for a reaction is possible to produce comparable results compared to batch by elongating the length of the reaction tubing.[4] All flow systems contain a solvent/reagent delivery system, mixer and reactor components. Comparatively, batch reactions may need to be set up in a glove box or with the use of a Schlenk line, whose use is arguably more cumbersome than what is needed for a flow setup.

The application of continuous flow in polymer synthesis is not novel. Szwarc first described the use of continuous flow as a means for the development of high throughput anionic polymerizations over 50 years ago.[1] The utility of continuous flow chemistry all but laid dormant for decades until the development of CRP reactions. For instance, atom transfer radical polymerization (ATRP) reactions have successfully been performed where the reaction tubing of the continuous flow reactor was subjected to light exposure to facilitate the activation, or initiation step of the ATRP reaction (Figure 1).[5] Furthermore, reversible addition-fragmentation chain-transfer polymerization (RAFT) reactions have been adapted to continuous flow conditions where a two block copolymer was synthesized through the utilization of two segments of reaction tubing.[6] The success of performing both ATRP and RAFT polymerization reactions under continuous flow

conditions suggests that the method could be extended to accommodate a ROMP reaction.

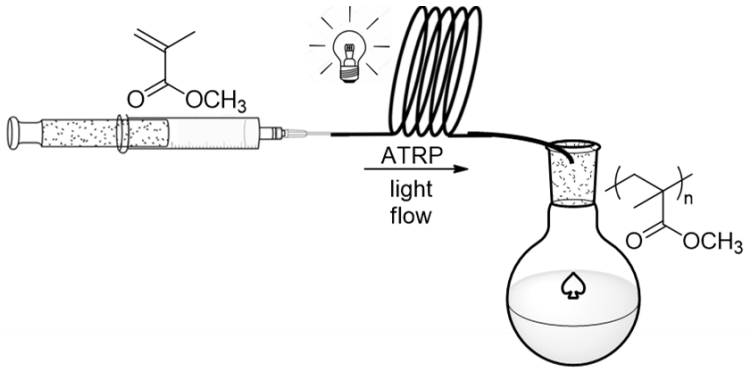

Figure 1. ATRP in flow with light source.

Continuous flow methods have also been coupled with batch reactions to synthesize designer macromolecules. In a recent study, Guironnet's group utilized continuous flow to perform ring opening polymerizations (ROP) with a norbornene-based initiator. The resulting macromonomers were then polymerized via ROMP in batch to generate bottle brush copolymers (Figure 2).[7] In another study, unsymmetrical cyclooctenes were functionalized through a two-step continuous flow procedure, but again the ROMP was performed under standard batch conditions in a grafting-through method (Figure 3).[8] In terms of metathesis polymerizations performed under continuous flow, both RCM and CM reactions have been successfully performed by Buchmeiser's laboratory,[9] which supports the idea that ROMP that can be adapted to flow reaction conditions.

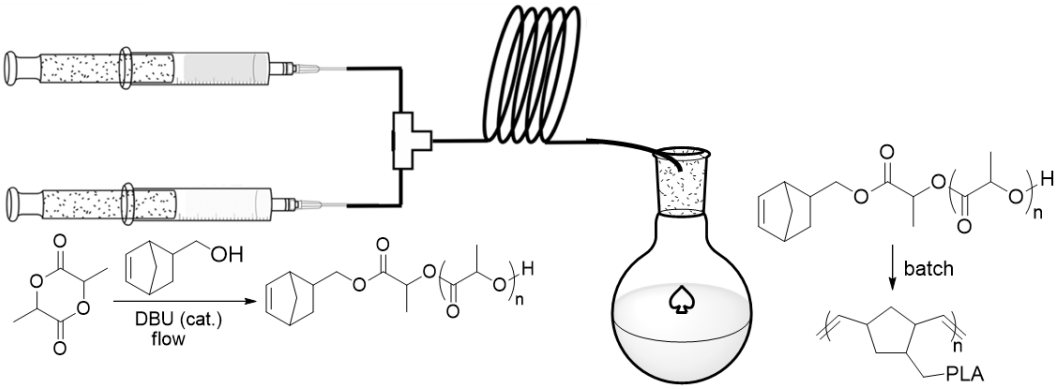

Figure 2. Continuous flow ROP followed by batch ROMP to synthesize bottle brush polymers.

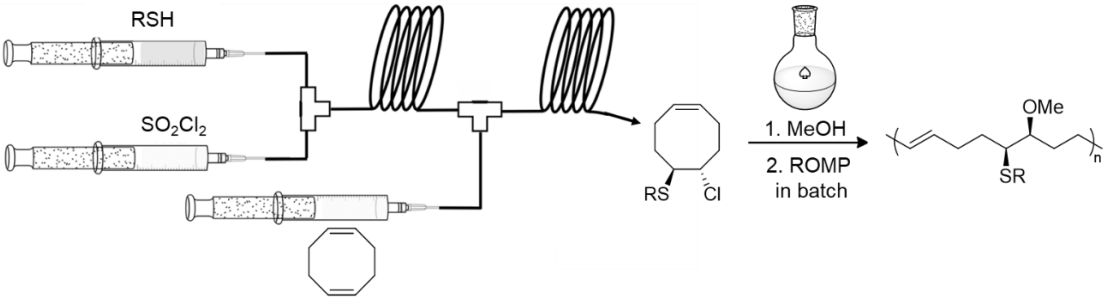

Figure 3. Synthesis of unsymmetrical cyclooctenes in flow, followed by ROMP in batch.

1.3 Olefin metathesis

Although the "olefin metathesis method" was only recognized by the Royal Swedish Academy of Sciences with the Nobel Prize 15 years ago, this reaction has been an academic and industrial curiosity for more than half a century.[10] The name 'metathesis' is derived from the Greek word for 'transposition', because the reaction resembles two alkenes simply swapping "R groups" (Figure 4). The mechanism for an equilibrium olefin metathesis reaction is slightly more complex than this. Chauvin first proposed the addition of the catalyst to the alkene bond of the starting material to form a metallocyclobutane intermediate that subsequently ring opens to form new alkene bonds through a [2 + 2] cycloaddition (Figure 5).[11] However, many of the catalysts used to carry

out these reactions were ill-defined. The groups of Grubbs and Schrock were responsible for preparing the first "well-defined" catalysts based on ruthenium, molybdenum and tungsten; ruthenium centered catalysts specifically have been coined as Grubbs-type catalysts or initiators (Figure 6). These catalysts can be used to carry out ring closing metathesis[12] (RCM) (Figure 7), cross metathesis[13] (CM) (Figure 8), and ROMP reactions (Figure 9); for these discoveries, Grubbs, Schrock and Chauvin were awarded the 2005 Nobel Prize in Chemistry.

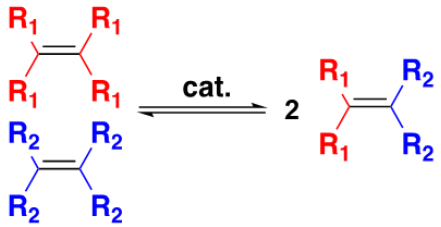

Figure 4. Cartoon depiction of olefin metathesis.

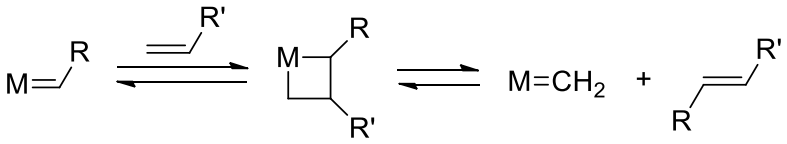

Figure 5. Olefin metathesis mechanism.

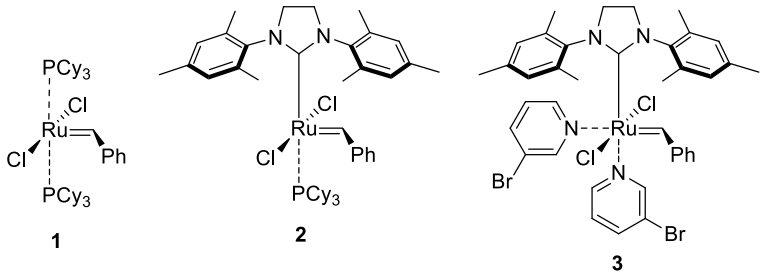

Figure 6. Chemical structures of Grubbs 1st Generation (**1**), Grubbs 2nd Generation (**2**) and Grubbs 3rd Generation (**3**) catalysts.

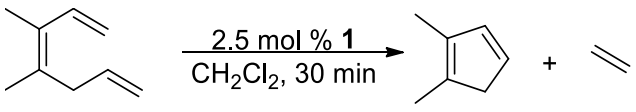

Figure 7. Example of a ring closing metathesis reaction.

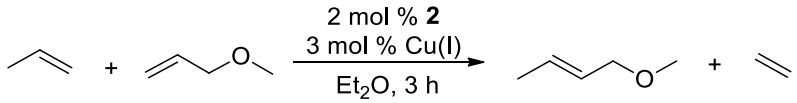

Figure 8. Example of a cross metathesis reaction.

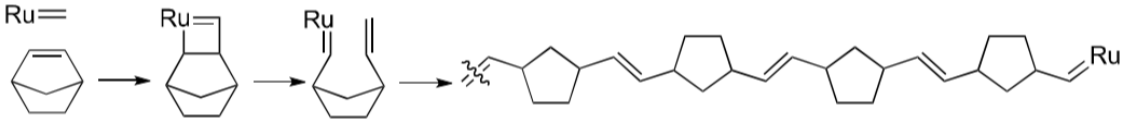

Figure 9. Ring opening metathesis polymerization (ROMP) abbreviated mechanism.

1.3.1 Release of ring strain as driving force for ROMP

Two major forms of strain that are alleviated through a ROMP reaction are angle and torsional strain about the alkene bond of the monomer. Torsional, or twisting, strain about the double bond exists due to the inability of free rotation within the confines of a cyclic molecule; torsional strain for cycloalkenes such as norbornene (**4**) are described in reference to the double bond of the ring. Norbornene has a ring strain value of 27.2 kcal/mol, more than double the 13.3 kcal/mol ring strain value of cyclooctadiene;[14] but both molecules readily polymerize via ROMP. Generally speaking, polymerization is almost always an entropically-disfavored process because of the high levels of order needed to convert multiple molecules of monomer into just a few molecules of polymer. ROMP can overcome this entropy issue because the release of ring strain is sufficiently large -to keep the reaction favored.

1.3.2 Norbornene derivative monomers

ROMP is also a very versatile polymerization reaction due to its ability to be performed using monomers that are cyclic with high ring strain values and contain an alkene bond. For instance, disubstituted norbornene rings have been polymerized in two steps with Grubbs-type catalysts as initiator to generate block copolymers with tailored

functionality (Figure 10).[15] In another study, functionalized cyclooctadiene was polymerized further showing how ROMP can be used to polymerize different monomers (Figure 11).[16]

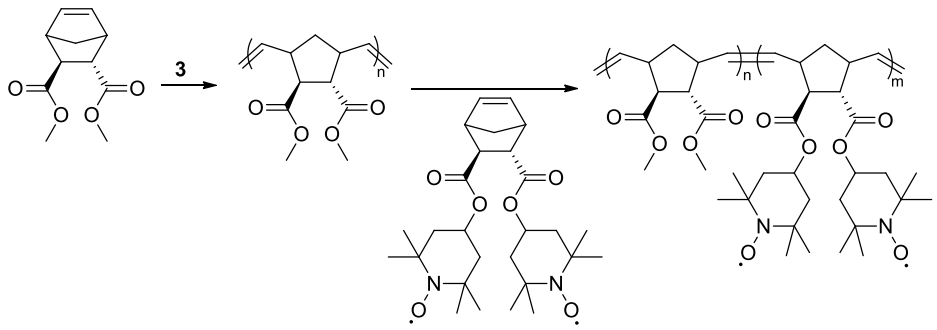

Figure 10. ROMP in batch with initiator **3** to generate block copolymer.

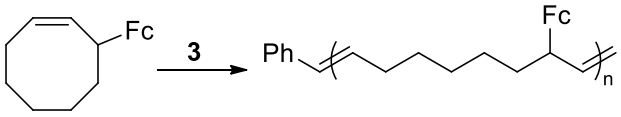

Figure 11. Functionalized cyclooctene ROMP polymerized with initiator **3**. Note: Fc is ferrocene.

Norbornene and oxa-norbonene derivatives can be highly functionalized and still successfully undergo ROMP in the presence of the Grubbs initiator. In an extensive 2003 study by Grubbs, his research group performed ROMP reactions on norbornene derived monomers under batch conditions utilizing ruthenium catalysts. Polydispersity index (*Đ*) values (described in section 1.4) reported were 1.10 or less indicating a high degree of control for the ROMP reaction.[17] This study is one of many that exemplifies how reaction conditions for performing ROMP as a "living" polymerization reaction have been optimized to achieve high control in the decades since its discovery.

1.3.3 Development of metathesis catalysts

Catalysts tailored to facilitate olefin metathesis date back to the mid-1900s and contained metal centers such as titanium,[18] tungsten,[19] and molybdenum[20] (Figure 12).

Although these species exhibited high catalytic activity, they were limited in their application due to low functional group tolerance and were highly sensitive to oxygen and moisture, rendering them difficult to handle in a laboratory setting.

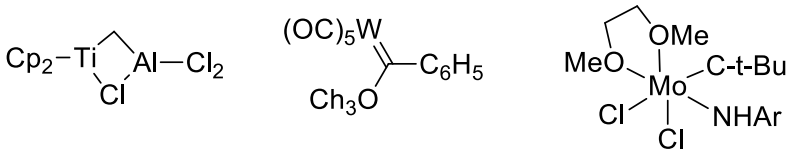

Figure 12. Early metathesis catalysts with Ti, W and Mo metal centers.

Because of the lack of functional group tolerance and moisture sensitivity of early transition metals, ruthenium-centered catalysts were found to be highly tolerant of different functional groups on the monomers. Additionally, they were oxygen tolerant, allowing for more ease of use. A ruthenium carbene species was experimentally found to be the active species for polymerizations through observation of a stable propagating carbene system using kinetic studies.[21] Grubbs (among others) went on to develop and define three generations of ruthenium-centered catalysts containing a carbene bond on the ruthenium center that participates in the initiation step of the olefin metathesis polymerization reactions, Grubbs 1st Generation (**1**), Grubbs 2nd Generation (**2**), and Grubbs 3rd Generation (**3**) are found in Figure 6. Even initiator **1** demonstrated greater functional group tolerance than other transition metal catalysts previously designed for olefin metathesis (Figure 13).

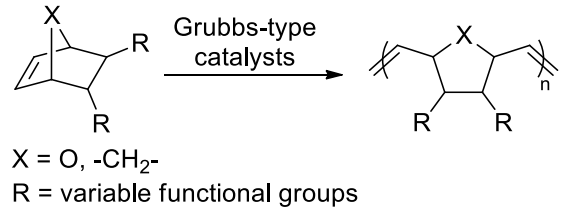

Figure 13. Variability of functionality on ROMP monomers with use of Grubbs-type catalysts.

Initiator **2** differs from **1** in that the PCy_3 ligand is replaced through a substitution reaction to add the N-heterocyclic carbene (NHC) ligand named SIMes, a saturated variant of the IMes ligand described by Arduengo (Figure 14).[22] Use of the NHC ligand resulted in a more efficient initiator to achieve the RCM of sterically hindered dienes.[23] Initiator **2** could also achieved ROMP of low-strained monomers.[24] Initiator **3** was designed to be a faster initiator compared to initiator **2** or **1** initiator by replacing the PCy_3 ligand with a more labile pyridine ring in solution.[25]

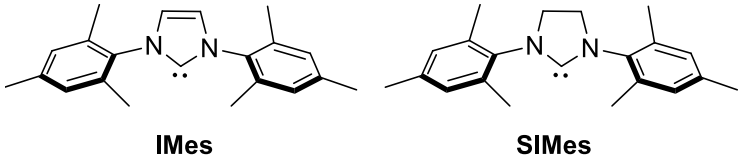

Figure 14. IMes and saturated SIMes NHC ligand of **2** and **3**.

1.3.4 Oxygen exclusion

Oxygen exclusion is necessary for living polymerization reactions to preserve the reactivity of the initiator. Since Grubbs-type initiators are much more tolerant of moisture and air than Schrock-type initiators,[26] a flow set up should provide a sufficiently closed system and a short enough reaction time to negate the need to deoxygenate the solutions prior to polymerization. A major benefit to flow chemistry is the ability to fine tune the length of time the monomer reacts with initiator in the reaction tubing, and consequently control the amount of time for polymerization. Within the reaction tubing of a flow system, a small quantity of monomer and initiator reacts at a time. Since the mass amount of monomer and the reaction time needed to fully polymerize are directly correlated, high conversions can be achieved in a shorter reaction time with flow. Batch reactions are limited in the sense that they need a sufficiently long reaction time to fully polymerize all

monomer present in the reaction vessel.

1.4 Polymer characterization terminology (M_n, M_w, $Đ$)

Typical polymerization reactions consist of three steps: initiation, propagation and termination. “Living” polymerization reactions differ in that there is a negligible amount of termination. Some event must transpire for a “living” chain to be “killed” (such as addition of a quenching agent to cleave the reactive terminal, or omega, end of a polymer chain). When characterizing a synthesized polymer, it is necessary to have a method to quantify how controlled the living polymerization reaction was performed. In a ROMP reaction, each molecule of Grubbs-type catalyst contains the ruthenium-carbene bond that reacts with a molecule of monomer to initiate the polymerization; each molecule of catalyst can initiate only one polymer chain. Consequently, if a large [M]:[I] is used for a reaction, polymer chains of a larger molecular weight would be generated. Using a smaller [M]:[I] would result in more initiations comparatively and generate shorter polymer chains since there is a finite quantity of monomer to react in the reaction flask.

Molecular weights of polymers are reported as an average weight value of all polymer segments in a sample; note all polymer segments are not exactly the same length due to initiations beginning at different points in time during the polymerization reaction. M_n stands for number-average molecular weight and equals the summation of the mole fraction of each polymer species times its molecular weight. M_w is the weight average molecular weight, a value that sums the weight fraction of each polymer species times its molecular weight. Consequently, M_w is always larger than M_n due to larger molecular weights contributing more to M_w calculations. The $Đ$ value is equal to the ratio of M_w/M_n and is always greater than 1.

$Đ$ is used to indicate the degree of uniformity in polymer weights or lengths of the sample. The more uniform the sample, the closer to 1.00 the value and the more narrow the Gaussian distribution of the chromatogram. Similarly, the more broad the molecular weight distributions, the larger the $Đ$ value. In theory, if a 200:1 [M]:[I] was used for the polymerization reaction, the polymer chains produced should have averaged to be 200 monomer lengths long. However, if the initiator decomposed prior to polymerization as is possible under ambient conditions, larger M_n values would be expected because the [M]:[I] increased.

$$Theoretical\ Mn = MW\ of\ monomer * monomer\ ratio\ value \qquad (1)$$

In equation (1), theoretical M_n is the value we anticipate for molecular weight if the ROMP flow reaction occurred perfectly and all polymer chains were the same length (monodisperse, $Đ$=1), "MW" is the molecular weight and the "monomer ratio value" is the ratio value of monomer that reacted with 1 equivalent of initiator. Note actual M_n values are typically rounded to the hundreds place due to the inability of the instrument to report on the polymer values more precisely with confidence. Polymers are typically classified as shown in Table 1.

Table 1. Polymer size classification based on $Đ$ values.

Type of polymer	***Đ* value**
Monodisperse	1
Narrow distribution	Less than 1.2
Medium width distribution	Between 1.2 and 3

Note that polymer chemists aim to achieve a narrow distribution for their polymer, but polymers with a medium width distribution are most common. Optimization

of experimental parameters can lead to a lower percent error between the theoretical and actual M_n values and a $Đ$ value less than 1.2.

Gel permeation chromatography (GPC) is a type of size exclusion chromatography (SEC). GPC is a method of liquid chromatography in which there is a stationary (solid) phase and a mobile (liquid) phase. The GPC instrument provides a means of *physical* partitioning of the sample tested based on the variety of sizes of the components that comprise the sample, but tells nothing of the *chemical* properties of the sample. Through GPC analysis M_n, M_w and $Đ$ values are determined.

1.5 "Click" reactions

The concept of click chemistry was developed and defined by Sharpless and was coined to describe reactions that are high yielding, atom economical and "green".[27] The prototypical "click" reaction is the copper-catalyzed azide/alkyne cycloaddition (CuAAC) reaction (Figure 15).[28] However, this is not the only "click" reaction that has been developed. For instance, strain-promoted alkyne azide cycloaddition (SPAAC) is another "click" process with a major difference from CuAAC in that it does not require copper catalysts (Figure 16).[29] There is also the thiol-ene Michael "click" reaction where a thiol reacts with the alkene in the presence of an amine to generate a thiol functionalized product (Figure 17).[30] Furthermore, Diels-Alder reactions are considered "click" reactions (Figure 18).[31]

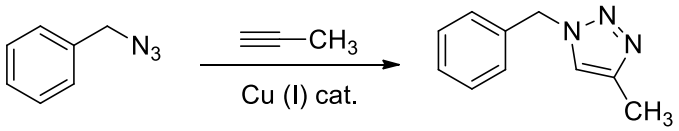

Figure 15. Example of a CuAAC "click" reaction.

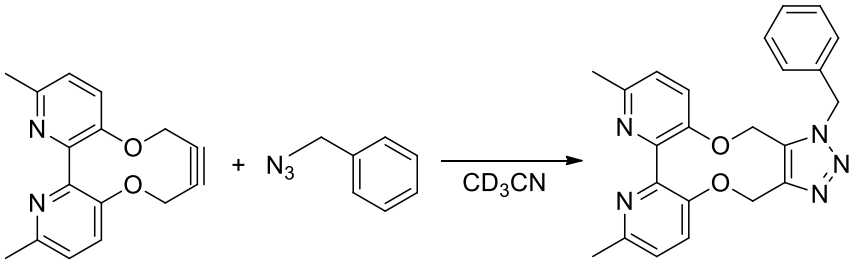

Figure 16. Example of SPAAC "click" reaction.

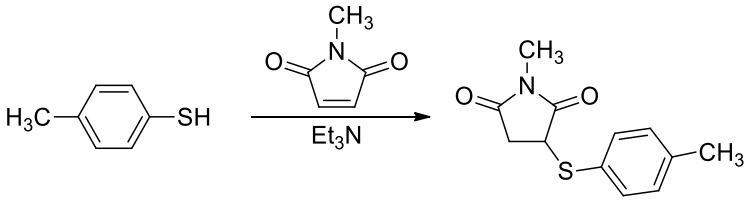

Figure 17. Example of thiol-ene Michael "click" reaction.

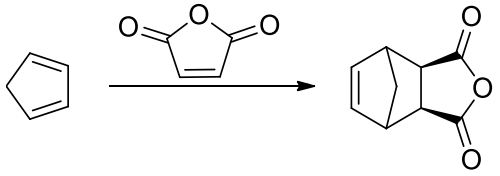

Figure 18. Example of Diels-Alder "click" reaction.

The nucleophilic substitution between thiols and α-bromo esters (dubbed a "thio-bromo click reaction") was first described by Percec for the synthesis of dendrimers and dendritic polymers.[32] Since the initial reports, the use of this strategy to modify polymers derived from ATRP and RAFT has been explored.

There is interest in the utilization of a thio-bromo "click" reaction as a tool for the post-polymerization modification of materials derived from ROMP.[33–35] They are especially useful to transform polymeric materials since their high yield suggests all functional groups can be reacted to have a new functionality by utilizing click processes.

Furthermore, since click reactions are somewhat "green" the amount of chemical and solvent waste generated can be minimized.

Previous publications of the Hobbs research group included research where thio-bromo "click" reactions were performed as a post-polymerization strategy on ROMP-derived monomers. Hobbs' laboratory has utilized this strategy for the modification of polymers derived from norbornene and cyclooctene derivatives. Furthermore, they have applied "click" chemistry to the development of polymers that are useful for drug delivery[34] (Figure 19) or can act as flame-retardants.[36] Recently, they have shown that these transformations can be carried out under solvent-free and mechanochemical reaction conditions where the polymerization is performed under batch conditions and followed by quenching using ethyl vinyl ether (EVE). The polymer, thiol and triethylamine was then placed in a ball mill where mechanical force drove the click reaction forward (Figure 20).[37] It was a goal to utilize a "one-pot synthetic procedure" to perform these thio-bromo "click" reactions, which could easily be extended to a continuous flow setup by addition of subsequent reaction tubing and allowing the reaction to proceed *in situ*.

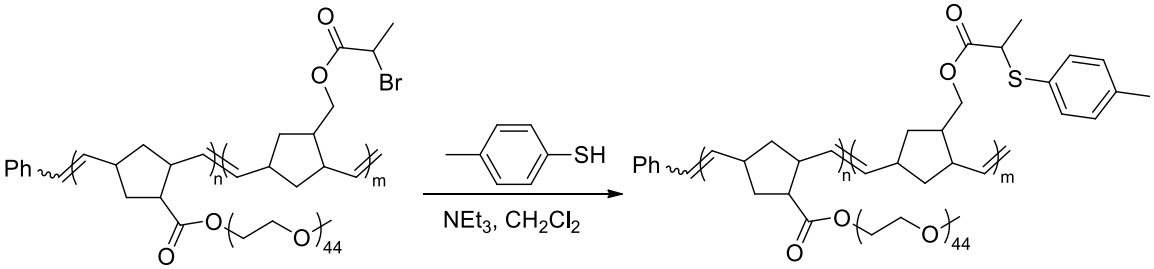

Figure 19. Thio-bromo "click" post-polymerization modification on polymerized bottle brush block copolymers.

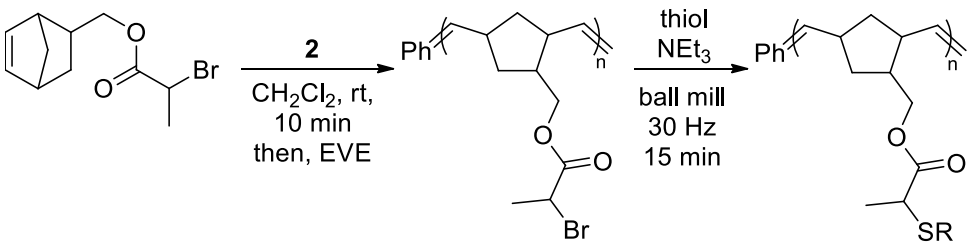

Figure 20. ROMP followed by mechanochemical thio-bomo "click" reaction.

1.6 Aim of this research

Polymerization reactions are often performed under batch conditions and have been optimized to obtain polymer chains of low dispersity and desired molecular weights. The main target of this research was to develop a process to perform ROMP reactions under continuous flow conditions using norbornene derived monomers. In order to achieve this, it was necessary to first optimize reaction conditions such as concentration of reactants and flow rate, and determine appropriate reagents. Optimized continuous flow reaction conditions were then adapted to generate homopolymers and block copolymers. It was a goal to use continuous flow to perform post polymerization thio-bromo click reactions *in situ* with adapted optimized reaction conditions.

CHAPTER II

Materials and Methods

2.1 General

All reagents and chemicals were purchased and used as received from commercial sources (Alfa Aesar Chemicals, Sigma Aldrich, TCI Chemicals). Continuous flow was performed using a dual syringe pump (Harvard Apparatus Model 22 or Harvard Apparatus) for synthesis of the homopolymers. A monosyringe pump (Cellpoint Scientific Inc.) was utilized in addition to the dual syringe pump to polymerize the block co-polymers and to perform the thio-bromo click reactions under flow conditions. Plastic (laboratory-grade polypropylene and polyethylene resin) syringes (13 mm diameter) with tubular reaction loop of 92 cm length polymer tubing (outer diameter x inner diameter (OD x ID): 1/16 x 0.04, IDEX Health and Science) were connected to a T-mixer (1/16 in PEEK 0.040 thru, IDEX Health and Science). Two segments of inlet tubing of 14 cm length were connected to the T-mixer on one end and the plastic syringes on the other (Figure 21).

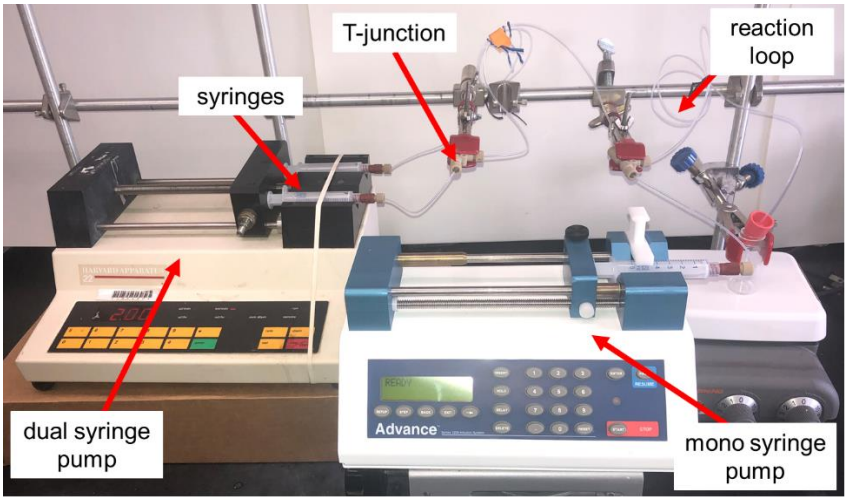

Figure 21. Experimental set-up for continuous flow reactions.

All reactions were quenched in 1 mL of ethyl vinyl ether. Solvent was removed using a vacuum pump, and a crude ^{1}H NMR spectra was obtained. The polymer products were washed with methanol and dried prior to calculating yields. The polymer was subsequently precipitated in methanol and dried under vacuum prior to preparing a 2 mg/mL sample used for GPC analysis.

^{1}H and ^{13}C NMR spectra were recorded on a Jeol NMR^{300} instrument, operating at 300.53 MHz. Chemical shifts are reported in in δ (ppm) relative to ^{1}H ($CDCl_3$: δ 7.26) and ^{13}C ($CDCl_3$: δ 77.23). The splitting patterns are designated as s (singlet); d (doublet); t (triplet); q (quartet); dd (doublet of doublets); td (triplet of doublets); m (multiplet); bs (broad singlet). Gel Permeation Chromatography (GPC) analysis was conducted on a Viscotek VE 1122 solvent delivery system and VE 3580 RI detector with LT4000L mixed column and molecular weight data were calculated relative to polystyrene standards.

Percent (%) conversion of monomer was ascertained through ^{1}H NMR integration analysis. Integral ratios of the post polymerization spectra analyzing the disappearance of the monomer and the appearance of the expected broad polymer peaks gave percent yield values. GPC was used to determine M_n and $Đ$ values. Furthermore, the block copolymerizations were analyzed by overlaying the GPC traces.

2.2 Synthesis

Synthesis of Grubbs 3rd Generation Catalyst (3).[38] Commercially available Grubbs 2nd Generation Catalyst (0.1000 g, 0.1180 mmol, 1.000 equiv) was added to a 20 mL vial equipped with a stir bar. Once the vial was clamped under the hood on a stir-plate, 2-bromopyridine (0.3927 g, 2.490 mmol, 21.20 equiv) was added dropwise using a

glass pipette. The reaction was stirred for 20 minutes. Pentane (10 mL) was added and stirred for 5 minutes until the product precipitated. Using a Buchner funnel, the reaction mixture was vacuum filtered to obtain a bright green solid powder (0.0863 g, 82.6% yield). The product was stored at 4 °C and utilized within 48 hours of synthesis.

Synthesis of monomers. Figure 22 shows the monomer scope of this study and Figure 23 shows the synthesis of the monomers.

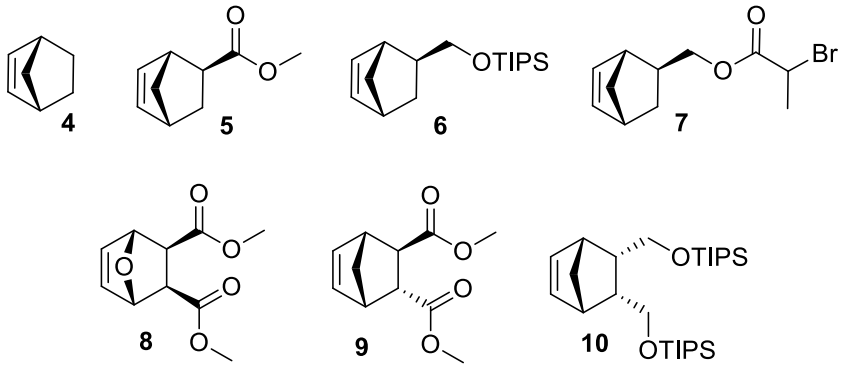

Figure 22. Monomer scope of this study.

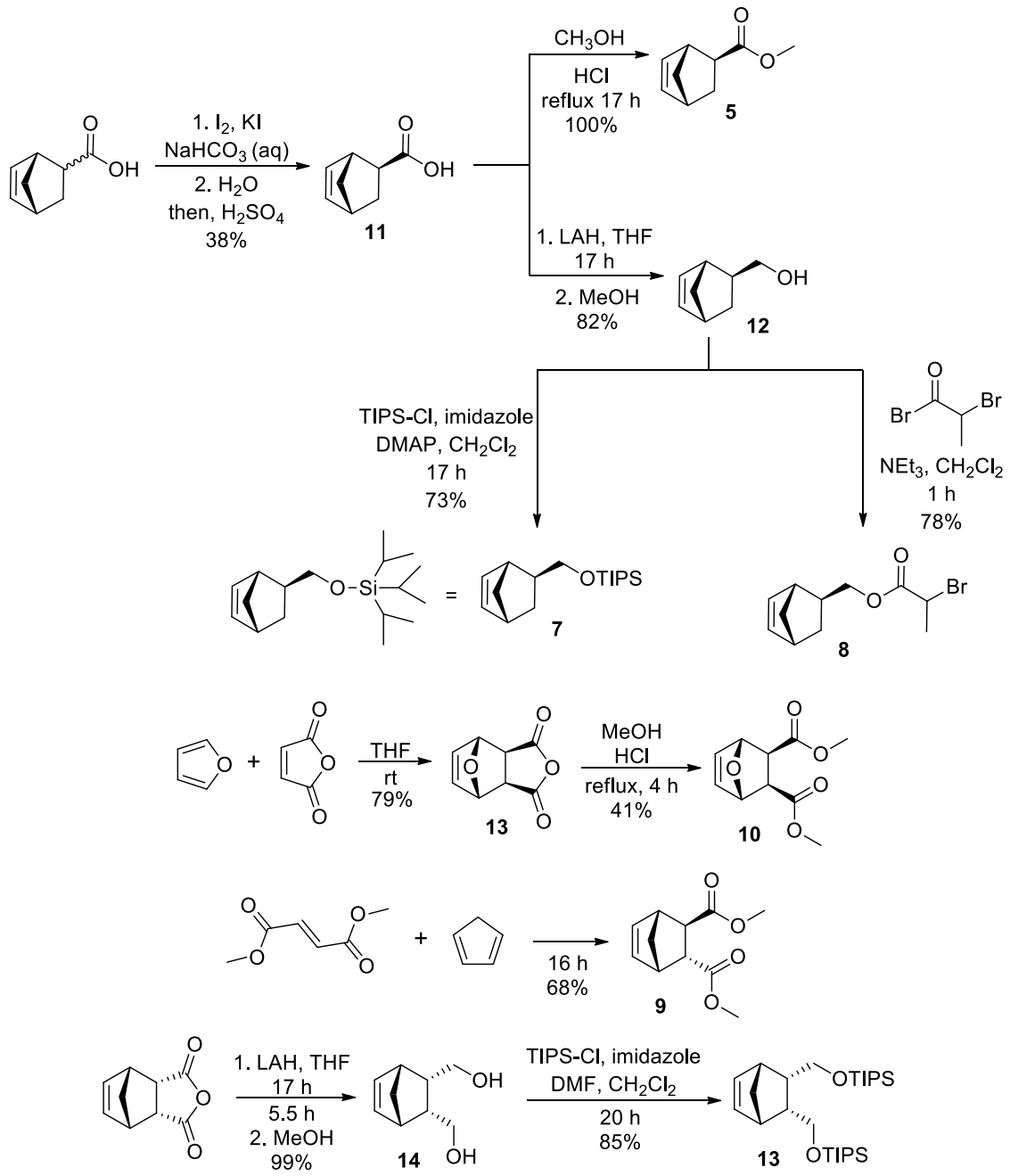

Figure 23. Synthesis of norbornene derived monomers.

Synthesis of exo-2-norbornene-5-carboxylic acid (11).[39] A 7:3 *endo*:*exo* mixture of 2-norbornene-5-carboxylic acid (4.00 g, 29.0 mmol, 1.50 equiv.) in aqueous $NaHCO_3$ (2.68 g, 31.8 mmol, 1.60 equiv, 0.800 M) was added to a 250 mL round bottom flask equipped with a stir bar. In a 150 mL Erlenmeyer flask, an aqueous solution

containing I_2 (4.90 g, 19.4 mmol, 1.00 equiv) and KI (5.28 g, 31.8 mmol, 1.60 equiv) in 80 mL of DI water was prepared and added three times. Using an addition funnel, the I_2/KI solution was added dropwise to the stirring round bottom flask containing the 2-norbornene-5-carboxylic acid until the solution retained a dark brown color. The mixture was filtered and transferred to a 250 mL separatory funnel. The solution was washed with diethyl ether (5 x 120 mL). Next, the aqueous layer was discolored using dropwise addition of 10% $Na_2S_2O_3$. The clear solution was acidified to a pH of 2 using 1 N H_2SO_4 and verified using pH paper. The product was extracted with diethyl ether in a 250 mL separatory funnel (4 x 120 mL). The combined organic layers were dried over Na_2SO_4. Solvent was subsequently removed under reduced pressure to yield pure solid product of an off-white color (1.14 g, 37.5% yield). ^{1}H NMR (301 MHz, $CDCl_3$) δ 6.14 (m, 2H), 3.11 (s, 1H), 2.94 (s, 1H), 2.27 (m, 1H), 1.95 (m, 1H), 1.54 (d, 1H), 1.40 (m, 2H).

Synthesis of methyl *exo*-2-norbornene-5-carboxylate (5).[40] *Exo*-2-norbornene-5-carboxylic acid (1.00 g, 7.20 mmol, 13.6 equiv), methanol (0.88 mL, 21 mmol, 40 equiv) and DCM (2.1 mL) was added to a 25 mL 2-neck round bottom flask equipped with a stirbar. Next, a catalytic amount of concentrated sulfuric acid (4 drops) was added dropwise to the stirring solution. The reaction mixture was refluxed using an oil bath and condenser for 17 hours. The reaction mixture was then cooled to room temperature and added to an 80 mL separatory funnel. The round bottom was rinsed with DCM (15 mL). The organic layer was washed with DI water (3 x 15 mL). Next, the organic layer was washed with saturated $NaHCO_3$ (15 mL). The product was then dried over Na_2SO_4, filtered and all solvent removed under reduced pressure. The resulting viscous yellow oil (1.09 g, 100.% yield) was sufficiently dried under the Schlenk line prior to using. ^{1}H

NMR (301 MHz, $CDCl_3$) δ 6.12 (dd, 1H, J = 5.6, 2.7 Hz), 6.09 (dd, 1H, J = 5.6, 3.1) 3.62 (s, 3H), 3.02 (s, 1H), 2.94 (s , 1H), 2.25 (dd, 1H, J = 9.2, 4.4), 1.93 (dt, 1H, J = 11.6, 9.2, 3.6), 1.48-1.52 (m, 2H), 1.30-1.45 (m, 2H).

Synthesis of *exo*-5-norbornene-2-methanol (12).[11] *Exo*-2-norbornene-5-carboxylic acid (**11**) (1.14 g, 8.25 mmol, 1.00 equiv) was added to a flame dried 50 mL 2-neck round bottom flask under N_2 atmosphere equipped with a stir-bar. Next, THF (25 mL) was added. The round bottom was cooled with an ice bath to 0 °C on top of the stir plate. While stirring, lithium aluminum hydride was added in small increments allowing any bubbling to subside prior to another addition. The reaction mixture was left to stir for 17 hours. The cloudy grey solution was poured into a 150 mL round bottom flask to accommodate following solvent additions. Slowly, methanol (25 mL) was added slowly not allowing any bubbling to overflow the round bottom flask. Next, all solvent was subsequently removed under reduced pressure. Once dried, DCM (50 mL) was added to the round bottom and a spatula was used to dislodge any solid from the interior of the round bottom. The reaction mixture was then vacuum filtered and the filtrate evaporated to yield the clear viscous oil as product (0.84 g, 82% yield). ^{1}H NMR (301 MHz, $CDCl_3$) δ 6.08 (m, 2H), 3.70 (m, 1H), 3.54 (m, 1H), 2.82 (s, 1H), 2.74 (s, 1H), 1.64 (m, 1H), 1.30 (m, 3H), 1.12 (m, 1H).

Synthesis of triisopropyl silane (-TIPS) protected *exo*-5-norbornene-2-methanol (6).[41] *Exo*-5-norbornene-2-methanol (**12**) (2.00 g, 16.1 mmol, 1.00 equiv) was added with triisopropylsilyl chloride (3.14 g 17.7 mmol, 1.10 equiv) and imidazole (3.29 g, 48.3 mmol, 3.00 equiv) to a 250 mL round bottom flask equipped with a stirbar. DCM (80 mL) was added to the reaction flask and allowed to stir for 17 hours at room

temperature. The mixture was concentrated by removal of solvent under reduced pressure and transferred to the top of a short layer of silica gel and flushed with hexane. Fractions were collected and solvent was subsequently removed under reduced pressure to yield a clear viscous oil (3.30 g, 73.0% yield). ^{1}H NMR (301 MHz, $CDCl_3$) δ 6.15-6.22 (m, 1H), 5.97-6.12 (m, 1H), 3.71-3.85 (dd, 1H, J = 9.7, 6.2 Hz), 3.52-3.66 (t, 1H, J = 9.1 Hz), 2.82 (s, 2H), 1.53-1.72 (m, 2H), 0.98-1.43 (m, 21H), 0.87-0.96 (m, 2H).

Synthesis of *exo*-5-norbornene-2-bromopropionate (7).[42] *Exo*-5-norbornene-2-methanol (**12**) (0.49 g, 4.0 mmol, 1.0 equiv) and triethylamine (1.1 mL, 8.0 mmol, 2.0 equiv) was added to 15 mL of DCM in a 100 mL round bottom flask equipped with a stirbar and septum. Next, 2-bromopropionyl bromide (0.84 mL, 8.0 mmol, 2.0 equiv) was added dropwise through the septum using a syringe. The reaction was stirred for 1 hour. All solvent of the resultant mixture was removed under reduced pressure. Next, diethyl ether (20 mL) was added, and the solution vacuum filtered. The filtrate was then added to a 60 mL separatory funnel and washed with DI water (3 x 15 mL). The organic layer was then dried over Na_2SO_4 and filtered. All solvent of the filtered solution was removed under reduced pressure to result in a viscous yellow oil (0.81 g, 78% yield). ^{1}H NMR (301 MHz, $CDCl_3$) δ 6.09 (s, 2H), 4.32-4.52 (m, 1H), 4.16-4.32 (m, 1H), 3.99-4.12 (m, 1H), 2.86 (s, 1H), 2.62-2.85 (m, 2H), 2.21-2.45 (m, 2H), 1-61-1.98 (m, 3H), 1.10-1.43 (m, 2H).

Synthesis of furan-maleic anhydride adduct (13).[43] Maleic anhydride (20.00 g, 204.0 mmol, 1.000 equiv) was added to a 250 mL round bottom flask equipped with a stirbar. Diethyl ether (100 mL) was added and stirred until all maleic anhydride was fully dissolved. Furan (69.4 g, 1020 mmol, 5 equiv) was added to the reaction flask and

allowed to stir overnight. The next day, the solution was vacuum filtered and rinsed with diethyl ether to yield a white solid (26.78 g, 79.04% yield). ^{1}H NMR (301 MHz, $CDCl_3$) δ 6.54 (s, 2H), 5.48 (s, 2H), 3.18 (s, 2H).

Synthesis of oxa-norbornene-dimethyl-2,3-dicarboxylate (8).[44] Furan-maleic anhydride adduct (**13**) (4.00 g, 24.1 mmol) was dissolved in methanol (40 mL) and added to a 100 mL round bottom flask equipped with a stirbar. The solution was refluxed for 4 hours. Once the reaction flask was cooled to room temperature, it was immersed in an ice-bath to form crystals. After 10 minutes the flask was scratched with a spatula to promote crystal formation. The solution was vacuum filtered and washed with cold methanol leaving a solid white flaky powder (2.10 g, 41.1% yield). ^{1}H NMR (301 MHz, $CDCl_3$) δ 6.43 (s, 2H), 5.24 (s, 2H), 3.64 (s, 6H), 2.79 (s, 2H).

Synthesis of norbornene-dimethyl 2-*endo*, 3-*exo*-dicarboxylate (9).[45] First, 2-Butenedioic acid dimethyl ester (1.63 g, 11.3 mmol, 1.00 equiv) was added to a 15 mL round bottom flask equipped with a stirbar, covered with a septum and clamped in place over a stir plate. Cyclopentadiene (1.0 mL, 12 mmol, 1.1 equiv) was added through the septum using a syringe. The reaction solution was stirred at room temperature for 16 h. All solvent of the solution was removed under reduced pressure and resulted in a colorless oil (1.62 g, 68.2% yield). ^{1}H NMR (301 MHz, $CDCl_3$) δ 6.23 (dd, 1H, J = 3.2, 6.1 Hz), 6.02 (dd, 1H, J = 3.1, 6.0 Hz), 3.68 (d, 6H), 3.34 (t, 1H, J= 3.8 Hz), 3.27 (s, 1H), 3.19 (s, 1H), 2.68 (dd, 1H, J = 4.5, 1.7 Hz), 1.54-1.64 (m, 1H), 1.3-1.48 (m, 1H).

Synthesis of *endo*-5-norbornene-2,3-methanol (14).[46] In a 100 mL round bottom flask equipped with a stirbar, 5-norbornene-*endo*-5,6-dicarboxylic acid anhydride (1.25 g, 7.60 mmol, 1.00 equiv) was dissolved in 25 mL of THF. While stirring, lithium

aluminum hydride (0.59 g, 15 mmol, 2.0 equiv) was added in small increments allowing any bubbling to subside prior to another addition. The reaction mixture was left to stir for 5.5 hours. The cloudy grey solution was poured into a 150 mL round bottom flask large enough to accommodate addition of more solvent. Slowly, methanol (25 mL) was added slowly not allowing any bubbling to overflow the round bottom flask. Next, all solvent was removed under reduced pressure. Once dried, DCM (50 mL) was added to the round bottom and a spatula was used to dislodge any solid from the interior of the round bottom. The reaction mixture was then vacuum filtered and the distillate evaporated to yield the clear viscous oil as product (1.19 g, 98.9% yield). ^{1}H NMR (301 MHz, $CDCl_3$) δ 6.03 (t, 2H, J = 1.9 Hz), 3.64 (d, 2H), 3.44 (t, 2H, J = 9.9 Hz), 2.81 (d, 4H), 2.52 (d, 2H), 1.33-1.46 (m, 2H).

Synthesis of TIPS protected *endo*-5-norbornene-2,3-methanol (10).[46] *Endo*-5-norbornene-2,3-methanol (**14**) (1.39 g, 9.00 mmol, 1.15 equiv), TIPS-Cl (3.85 mL, 18.0 mmol, 2.00 equiv), imidazole (2.45 g, 36.0 mmol, 4.00 equiv) and 4.5 mL of dimethylformamide was added to a 100 mL round bottom flask equipped with a stirbar and was allowed to mix vigorously for 20 h. The reaction mixture was then poured into a 60 mL separatory funnel. Next, a 50% diethyl ether/hexane solution (20 mL) was added. The organic layer was washed with 1 N aqueous sulfuric acid (2 x 20 mL). The aqueous layer was subsequently removed, and the organic layer washed with saturated aqueous NaCl (2 x 20 mL). Lastly, the organic layer was dried over Na_2SO_4, filtered, and the solvent removed under reduced pressure to yield a clear viscous oil (3.58 g, 85.3% yield). ^{1}H NMR (301 MHz, $CDCl_3$) δ 6.08 (s, 2H), 3.48-3.2 (m, 4H), 3.28 (t, 2H, J = 1.3 Hz), 2.9 (s, 2H), 2.34 (s, 2H), 0.91-1.42 (m, 42H).

2.3 General procedure for continuous flow homopolymerizations

All homopolymerization reactions were performed utilizing these conditions unless otherwise specified (Figure 24). To a 6 mL, plastic (laboratory-grade polypropylene and polyethylene resin) syringe was loaded a solution of monomer (1.5 mmol) in CH_2Cl_2 (4 mL). Another 6 mL syringe was loaded with a solution of initiator **3** (0.0066 mmol) in CH_2Cl_2 (4 mL). The two syringes were then connected to the reaction loop, placed in the syringe pump, and subsequently pumped through the reaction loop at the appropriate flow rate corresponding to a specific residence time (Figure 25).

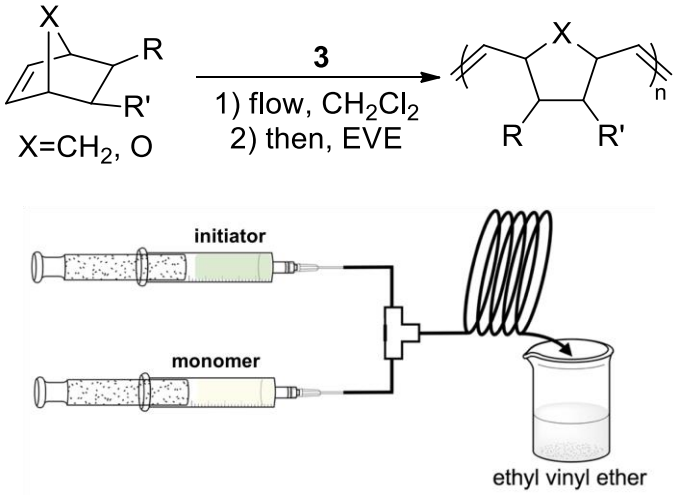

Figure 24. Generalized homopolymerization reaction (top) and cartoon schematic of experimental set-up for homopolymerization reactions (bottom).

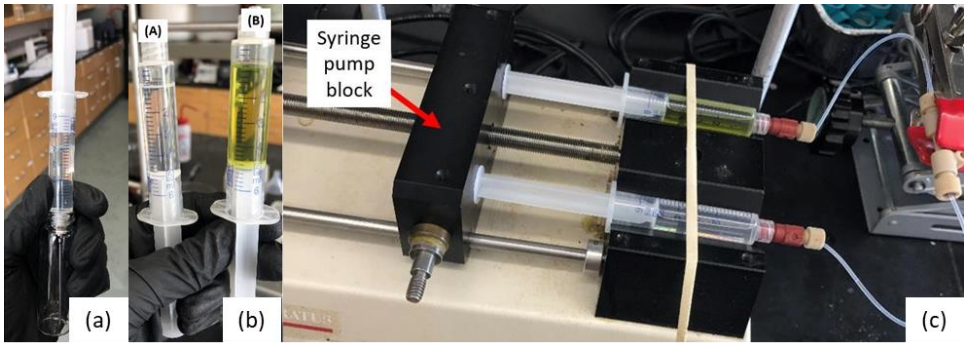

Figure 25. (a) Drawing 1 mL of air into monomer headspace; (b) syringes loaded with dissolved monomer (A) and initiator (B); (c) properly positioned syringe pump block.

Note that residence time is calculated by dividing the reaction tubing volume by the flow rate of the syringe pump. An example calculation is found below (Equation 3).

$$R_t = \frac{reaction\ tubing\ volume\ (mL)}{flow\ rate\ (\frac{mL}{min})} = \frac{0.75\ mL}{1.0\ \frac{mL}{min}} = 0.75\ min = 45\ s \qquad (3)$$

For experiments performed at 0 ^{o}C, the mixer and reaction tube reactor were submerged in an ice water bath. The product solution was collected in a vial of stirring ethyl vinyl ether (EVE) (1 mL) and stirred for a few minutes. To determine % conversion, ^{1}H NMR analysis was performed after excess solvent and ethyl vinyl ether were removed under vacuum. Purified product was obtained through solvent precipitation into methanol followed by characterization by ^{1}H NMR and GPC.

*Homopolymerization of **4**.* Monomer **4** was polymerized according to the general procedure outlined above. The product was isolated in 76% yield for 7.5 s. Product was isolated in 83% yield for t_R = 22.5 at 0 ^{o}C. ^{1}H NMR (300 MHz, $CDCl_3$) δ 5.35-5.25 (m, 1H), 5.2-5.15 (d, 2H), 2.85-2.7 (bs, 2H), 2.5-2.35 (bs, 1H), 1.9-1.7 (bs, 5H), 1.6-1.15 (m, 12H), 1.1-0.9 (bs, 2H). GPC analysis showed M_n = 44,200 g/mol and $Đ$ = 1.18 and M_n = 32,000 g/mol and $Đ$ = 1.14 at 0 ^{o}C for t_R = 22.5 and M_n = 36,500 g/mol and $Đ$ = 1.07 for t_R = 7.5 s.

*Homopolymerization of **5**.* Monomer **5** was polymerized according to the general procedure outlined above. The product was isolated in 77% yield for t_R = 7.5 s. ^{1}H NMR (300 MHz, $CDCl_3$) δ 5.4-5.1 (m, 2H), 3.7-3.6 (bs, 3H), 3.2-2.9 (m, 1H), 2.8-2.4 (m, 2H), 2.2-1.8 (m, 2H), 1.75-1.43 (bs, 2H), 1.4-1.1 (bs, 2H). GPC analysis showed M_n = 43,400 g/mol and $Đ$ = 1.30 for t_R = 22.5 and M_n = 34,900 g/mol and $Đ$ = 1.11 for t_R = 7.5 s.

*Homopolymerization of **5**$_{(endo/exo)}$.* Monomer **5**$_{(endo/exo)}$ was polymerized according to the general procedure outlined above. The product was isolated in 40% yield for t_R =

22.5 s. Product was isolated in 45% yield for t_R = 7.5 s. GPC analysis showed Mn = 11,000 g/mol and Đ = 1.67 for t_R = 22.5 and Mn = 22,000 g/mol and Đ = 1.57 for t_R = 7.5 s.

*Homopolymerization of **6***. Monomer **6** was polymerized according to the general procedure outlined above. The product was isolated in 86% yield for t_R = 7.5 s ^{1}H NMR (300 MHz, $CDCl_3$) δ 5.38-5.05 (m, 5H), 3.8-3.3 (m, 12H), 2.9-2.65 (bs, 2H), 2.6-2.3 (bs, 2H), 2.25-2.1 (bs, 1H), 1.95-1.65 (bs, 6H), 1.6-1.35 (bs, 10H), 1.3-1.2 (m, 1H). GPC analysis showed M_n =54,000 g/mol and $Đ$ = 1.16 for t_R = 22.5 and M_n = 68,300 g/mol and $Đ$ = 1.18 for t_R = 7.5 s.

*Homopolymerization of **7***. Monomer **7** was polymerized according to the general procedure outlined above. The product was isolated in 93% yield for t_R = 7.5 s. ^{1}H NMR (300 MHz, $CDCl_3$) δ 5.4-5.1 (bs, 2H), 4.45-4.3 (m, 1H), 4.25-3.9 (m, 2H), 3.0-2.8 (bs, 1H), 2.65-2.4 (m, 1H), 2.1-1.8 (m, 4H), 1.4-1.05 (m, 3H). GPC analysis showed M_n = 44,000 g/mol and $Đ$ = 1.33 for t_R = 22.5 and M_n = 45,200 g/mol and $Đ$ = 1.12 for t_R = 7.5 s.

*Homopolymerization of **8***. Monomer **8** was polymerized according to the general procedure outlined above. The product was isolated in 76% yield for t_R = 450 s. ^{1}H NMR (300 MHz, $CDCl_3$) δ 5.95 (s, 1H), 5.65-5.5 (bs, 2H), 5.23 (m, 1H), 5.15-5.0 (s, 2H), 4.7 (s, 1H), 3.8-3.6 (s, 10H), 3.5-3.0 (s, 3H), 1.7-1.5 (s, 7H), 1.4-1.25 (bs, 1H). GPC analysis showed and M_n = 52,000g/mol and $Đ$ = 1.24 for t_R = 450 s.

2.4 General procedure for continuous flow copolymerizations

All copolymerization reactions were carried out utilizing these conditions, unless otherwise stated (Figure 26). To a 6 mL plastic (laboratory-grade polypropylene and

polyethylene resin) syringe was loaded a solution of norbornene (**4**) (0.66 mmol) in CH_2Cl_2 (2 mL). Another 6 mL syringe was loaded with a solution of (**5**, **6**, or **7**) (0.0066 mmol) in CH_2Cl_2 (2 mL). The two syringes were then connected to the first segment of reaction loop. A third 6 mL syringe was loaded with a solution of monomer (0.66 mmol) and connected to the inlet tubing of the second segment of reaction loop and placed in the monosyringe pump. The solution of **3** was pumped through the first segment of reaction loop at a flow rate of 2 mL/min until the solution reached the second T-mixer at which point the monosyringe pump was turned on at a rate of 2 mL/min. The product solution was collected in a vial of stirring ethyl vinyl ether (1 mL) and was allowed to stir for a few minutes. To determine % conversion, ^{1}H NMR analysis was performed after excess solvent and ethyl vinyl ether were removed under vacuum. Purified product was obtained through solvent precipitation into methanol to remove any unreacted monomer and initiator followed by characterization by ^{1}H NMR and GPC.

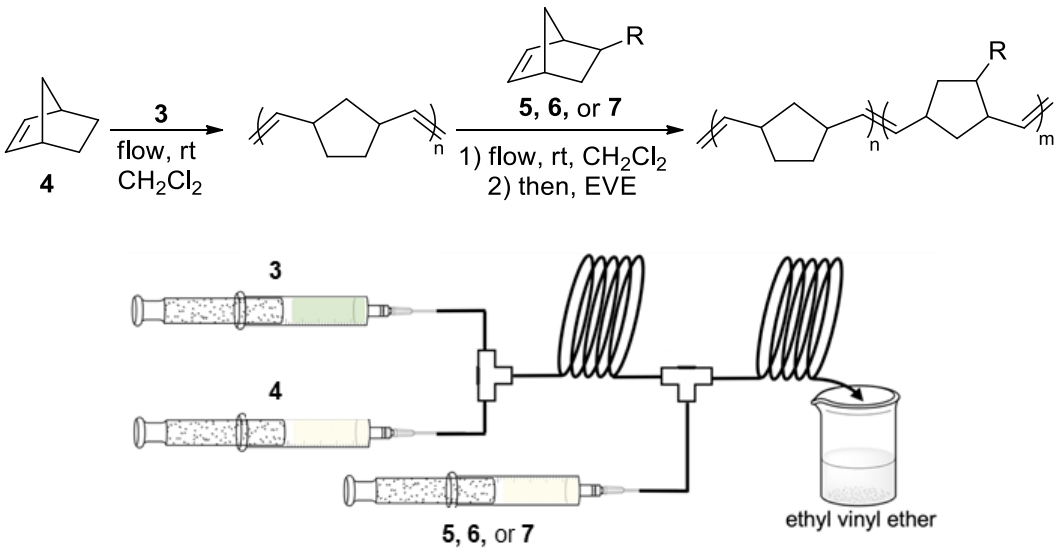

Figure 26. Generalized copolymerization reaction (top) and cartoon schematic of experimental setup for copolymerization reactions (bottom).

*Copolymerization of **4** and **5***. Monomers **4** and **5** were polymerized according to the general procedure outlined above. The product was isolated in 78% yield for t_R = 22.5 s for each loop. ^{1}H NMR (300 MHz, $CDCl_3$) δ 5.4-5.05 (m, 2H), 3.7-.55 (bs, 2H), 3.2-2.9 (bs, 1H), 2.9-2.3 (m, 2H), 2.1-1.45 (m, 4H), 1.4-0.8 (m, 3H). GPC analysis showed M_n = 35,600 g/mol and $Đ$ = 1.21.

*Copolymerization of **4** and **6.*** Monomers **4** and **6** were polymerized according to the general procedure outlined above. The product was isolated in 71% yield for t_R = 22.5 s for each loop. ^{1}H NMR (300 MHz, $CDCl_3$) δ 5.4-5.1 (m, 2H), 3.8-3.35 (m, 1H), 2.9-2.7 (bs, 1H), 2.65-2.1 (m, 1H), 2.0-1.65 (bs, 3H), 1.6-1.2 (m, 2H). GPC analysis showed M_n = 44,500 g/mol and $Đ$ = 1.25.

*Copolymerization of **4** and **7***. Monomers **4** and **7** were polymerized according to the general procedure outlined above. The product was isolated in 80% yield for t_R = 22.5 s for each loop. ^{1}H NMR (300 MHz, $CDCl_3$) δ 5.4-5.15 (m, 2H), 4.5-4.3 (m, 2H), 4.25-4.15 (m, 2H), 2.9-2.7 (bs, 2H), 2.6-2.3 (bs, 1H), 2.1-1.5 (bs, 18 H), 1.4-1.1 (m, 7H). GPC analysis showed M_n = 43,600 g/mol and $Đ$ = 1.27.

2.5 General procedure for continuous flow ROMP & thio-bromo "click" reactions

All thio-bromo click reactions were carried out utilizing these conditions unless otherwise specified. To a 6 mL plastic (laboratory-grade polypropylene and polyethylene resin) syringe was loaded a solution of monomer **7** (1.5 mmol) in CH_2Cl_2 (2 mL). Another 6 mL syringe was loaded with a solution of **3** (0.0066 mmol) in CH_2Cl_2 (2 mL). Those two syringes were then connected to the first segment of reaction loop. A third 6 mL syringe was loaded with a solution of thiol (**15, 16** or **17**) (4.5 mmol) (Figure 27) and triethylamine (4.5 mmol) in sufficient THF to create a total 2 mL volume (0.66 mmol)

that was then connected to the inlet tubing of the second segment of reaction loop and placed in the monosyringe pump (Figure 28). The monomer **7** and **3** solution were pumped through the first segment of reaction loop at 2 mL/min until the solution reached the second T-mixer at which point the monosyringe pump was turned on at a rate of 2 mL/min. The product solution was collected in a vial of stirring ethyl vinyl ether (1 mL) and was allowed to stir for a few minutes. To determine % conversion, ^{1}H NMR analysis was performed after excess solvent and ethyl vinyl ether were removed under gentle vacuum. Purified product was obtained through solvent precipitation into methanol to remove any unreacted monomer and inititor followed by characterization by ^{1}H NMR and GPC.

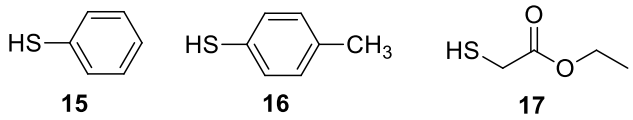

Figure 27. Thiols utilized to perform thio-bromo click reactions in flow.

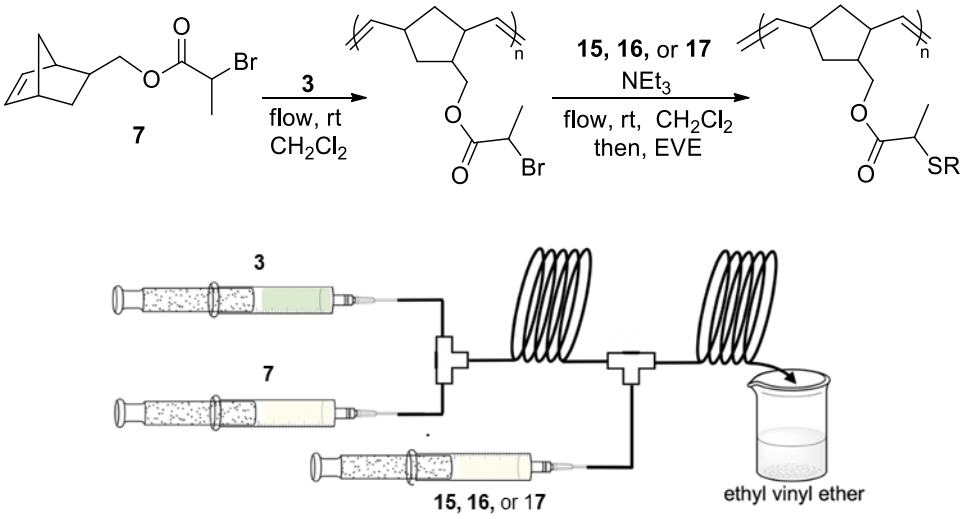

Figure 28. Generalized thio-bromo click reaction (top) and cartoon schematic of experimental set-up for thio-bromo click reactions (bottom).

*Thio-bromo click reaction of **7** with **15***. Monomer **7** was polymerized according to the general procedure outlined above, then reacted with **15**. The product was isolated in 78% yield for t_R = 22.5 s. ^{1}H NMR (300 MHz, $CDCl_3$) δ 7.5–7.3 (d, J 5 6.07 Hz, 1H), 7.3–7.18 (s, 2H), 5.5–5.0 (m, 2H), 4.42– 4.27 (t, J 5 71.79 Hz, 1H), 3.6–3.4 (s, 2H), 3.03–2.16 (m, 1H), 2.04–0.9 (m 5H). GPC analysis showed M_n = 48,800 g/mol and $Đ$ = 1.43.

*Thio-bromo click reaction of **7** with **16***. Monomer **7** was polymerized according to the general procedure outlined above, then reacted with **16**. The product was isolated in 82% yield for t_R = 22.5 s. ^{1}H NMR (300 MHz, $CDCl_3$) δ 7.48–7.3 (d, J 5 22.18 Hz, 1H), 7.2–7.0 (s, 1H), 5.38–5.08 (m, 1H), 4.13–3.71 (d, J 5 36.03Hz 1H), 3.78–3.6 (s, 1H), 3.58–3.42 (s, 4H), 3.02–2.5 (m, 3H), 2.08–0.91 (m, 7H). GPC analysis showed M_n = 41,700 g/mol and $Đ$ = 1.39.

*Thio-bromo click reaction of **7***. Monomer **7** was polymerized according to the general procedure outlined above, then reacted with **17**. The product was isolated in 74% yield for t_R = 22.5 s. ^{1}H NMR (300 MHz, $CDCl_3$) δ 7.5–7.3 (s, 1H), 5.49–5.1 (m, 9H), 4.3–3.8 (m, 13H), 3.6–3.57 (m, 3H), 3.5–3.414 (m, 13H), 3.37-3.239 (m, 3H), 3.13–2.69 (m, 5H), 2.6–2.24 (m, 4H), 2.10–1.53 (m, 12H), 1.52–1.38 (m, 9H), 1.36–1.04 (m, 18H).

2.6 ^{1}H NMR percent conversion determination

NMR spectroscopy is used in organic synthesis because it is a highly sensitive and powerful tool to verify product purity of synthesized monomers, as well as to calculate percent conversions for polymerization reactions.

2.6.1 Homopolymerizations and block copolymerizations

This study focused on the polymerization of norbornene derived monomers under continuous flow conditions. The alkene hydrogens on the norbornene ring appear around

6 ppm for *exo* norbornene isomer monomers. Once ROMP is done using the monomer, the product consists of a non-branched polymer chain (Figure 9). The hydrogens off of the alkene bonds in the polymer chain appear at about 5.0-5.5 ppm as a broad singlet. A broad peak is expected due to there existing a slightly different chemical environment for the functional groups appending off the carbon chain backbone of the polymer chain and the hydrogens off of the alkene bond of the ROMP generated product polymer. The spectrum for a polymer is the equivalent of a bunch of overlaid diastereomers. By obtaining the values of the integrated area from 5.0-5.5 ppm (correlating to the polymer alkene hydrogens) and comparing it in relation to the sum of the total integrated area from 5.85-6.2 ppm (correlating to the monomer alkene hydrogens) and the 5.0-5.5 ppm, a percent conversion of monomer to polymer can be obtained as shown in equation 2.

$$\frac{|integrated\ area\ of\ polymer\ peak|}{|integrated\ area\ of\ monomer\ peak + integrated\ area\ of\ monomer\ peak|} * 100 = \frac{|integrated\ area\ from\ 5.0 - 5.5\ ppm|}{|integrated\ area\ from\ 5.85 - 6.2\ ppm + integrated\ area\ from\ 5.0 - 5.5\ ppm|} * 100 \quad (2)$$

The same logic can be extended to calculate the percent conversion of monomer to block copolymer since the two monomers used are both norbornene derived monomers.

2.6.2 Thio-bromo "click" reactions

To quantify the percent conversion of the α-bromo ester functional group of **7** to thiol functionality (**15, 16** or **17**) on the polymer chain in the thio-bromo click reaction, the peak correlating to the α-carbon hydrogen can be integrated and compared (Figure 29).

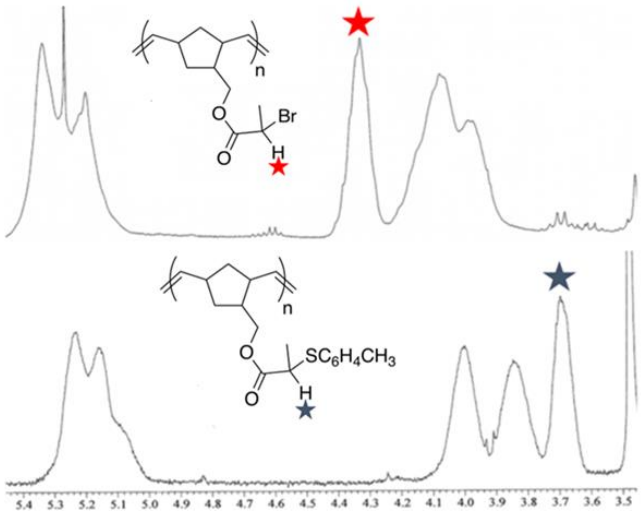

Figure 29. Overlaid spectra showing partial ^{1}H NMR spectra of polymer **4** before (top) and after (bottom) thio-bromo click modification.

The hydrogen of the α-bromo ester group of **7** appears at about 4.2-4.4 ppm, more downfield than the hydrogen of the less electronegative thio ether functional groups of **15, 16** and **17** which appears at about 3.6-3.75 ppm.

2.7 Precipitation methodology

To a 25 mL Erlenmeyer flask equipped with a stir bar, about 5-10 mL of methanol were added. The flask was clamped in place above a stir plate and set to stir at the fastest speed setting. In another vial, the crude product of the flow reaction was dissolved in minimal DCM (at most 1.5 mL). The crude product was fully dissolved ensuring the solution was viscous. The crude product solution was loaded into a disposable pipette and dropped slowly (one drop at a time in a controlled manner) into the stirring methanol. The methanol was in enough excess to allow the polymer to precipitate out of solution. The excess solvent (containing the unreacted monomer and initiator) was decanted, and the precipitate placed under vacuum on the Schlenk line to remove any residual solvent.

CHAPTER III

Results and Discussion

3.1 Optimizing reaction conditions

The goal of this research was to adapt ROMP to a continuous flow procedure. The initial experimental parameters included the use of initiator **2** to facilitate the ROMP of **4**. Initially, a 0.48 M solution of **4** and a 0.0024 M solution of **3** initiator was loaded into separate 6 mL plastic syringes affording a 227:1 [M]:[I] ratio. The syringes were connected to the flow set up and loaded into the dual syringe pump. The reaction was carried out using a flow rate of 1 mL/min, correlating to a residence time (t_R) of 45 s. Performing the flow homopolymerization of **4** with the aforementioned reaction conditions resulted in an extremely viscous polymer solution that clogged the reactor tubing, resulting in a product not able to be analyzed (Figure 30). This likely occurred due to the slower initiation rate of initiator **2**, which resulted in faster propagation to generate polymer chains higher molecular weights that could not be pumped out of the tubing.

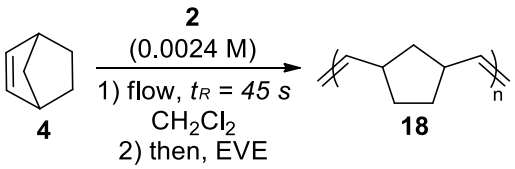

Figure 30. Initial reaction conditions of failed flow homopolymerization of **4** with initiator **2**.

To prevent future clogging of the flow reactor tubing, the experimental parameters were adjusted to use the faster-initiating **3** instead of **2.** Additionally, this initiator was used in more dilute reactions (0.38 M and 0.0019 M for the initial monomer ($[M]_o$) and initiator ($[I]_o$), respectively). Polymerization of **4** (with these corrections in

place) could successfully be carried out with a flow rate of 2 mL/min (t_R = 22.5 s) to provide **18** in >95% conversion (Table 2, Entry 1) (Figure 31).

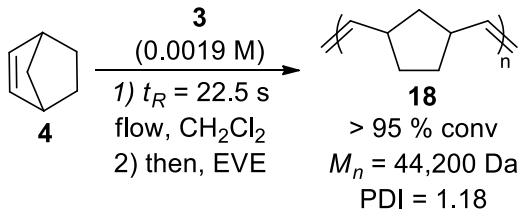

Figure 31. Optimized reaction conditions for successful flow homopolymerization of **4** with initiator **3**.

Next, GPC analysis was performed on the flow generated **18**. *Đ* was relatively low (1.18), but the M_n was much higher (44,200 Da) than the theoretical M_n (21, 372 Da) (Table 2, Entry 1). Grubbs and coworkers found that cooling the ROMP reaction to 0 °C could provide better control over molecular weight by retarding the propagation rate of the polymerization.[17] In flow, this can easily be achieved by simply submerging the reaction tubing and T-mixer in an ice-water bath. Indeed, this resulted in better control (M_n = 32,000 Da and *Đ* = 1.14) (Table 2, Entry 2) (Figure 32).

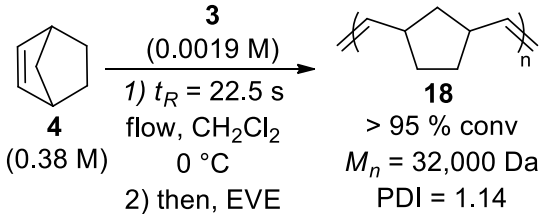

Figure 32. Improved flow homopolymerization of **4** with initiator **3** at 0 °C.

Table 2. Homopolymerizations under flow conditions

Monomer*	Conv.[a] (%)	$M_{n(\text{theor.})}$ Da	M_n[b] Da	*Đ*
4	>95	21 372	44 200	1.18
4[c]	>95	21 372	32 000	1.14

*Conditions: **M:I** = 227:1, $[\mathbf{M}]_0$= 0.38 M, $[\mathbf{I}]_0$= 0.0017 M, t_R = 22.5 s, tubular path length = 92 cm, room temperature. [a]Determined by ^{1}H NMR. [b]Determined by GPC. [c]t_R = 450 s.

3.2 *endo/exo* selectivity

With the successful flow generation of **18**, we next decided to carry out the ROMP of other norbornene derivatives under the optimized flow conditions at room temperature. The next experiment attempted utilized a commercially-available mixture of *endo* and *exo* (ca. 1:1) **5.** Results were somewhat discouraging, with a low conversion of only 35% from monomer to polymer (Table 3). Changing the flow rates and initial concentrations of the monomer and initiator solutions did not yield any substantial improvement in ^{1}H NMR calculated percent conversion values. Through analysis of the NMR spectra of the *endo*/*exo* mixture of **5** as monomer, (Figure 33, top) and comparing it to the NMR spectra of the generated polymer of **5** (Figure 33, bottom), it was discovered that the *exo* isomer of **5** polymerized under the flow conditions at a much more rapid rate than the *endo* isomer. Note that the rate at which *endo* versus *exo* isomers of a monomer can be polymerized is not typically an issue under batch polymerization reaction conditions since ample reaction time is allowed to elapsed to allow for both isomers to react to completion.

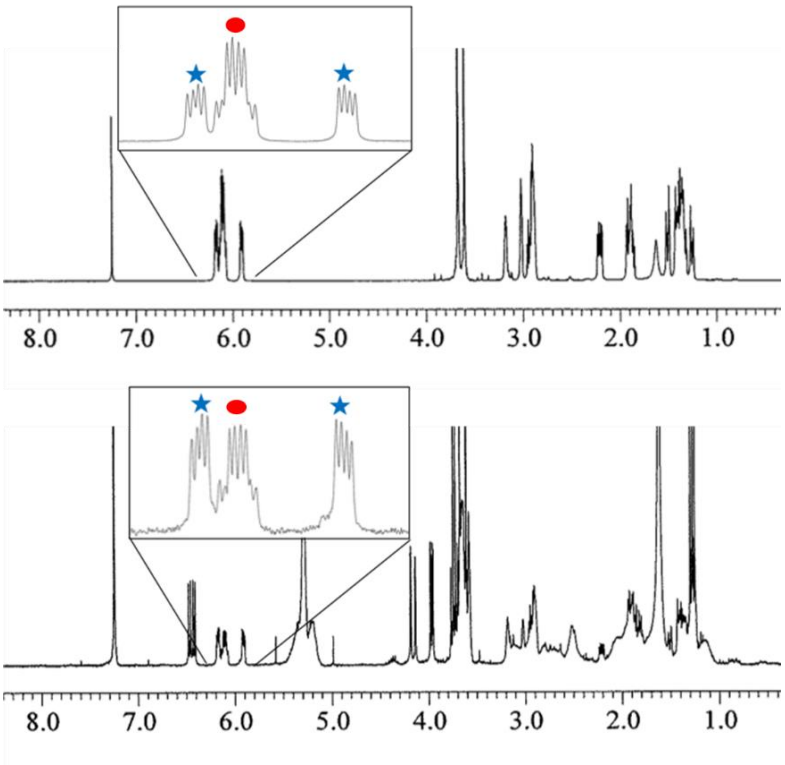

Figure 33. Partial ^{1}H NMR spectra of the commercially-available *exo/endo* monomer **5** (top) and the crude spectrum after polymerization (bottom). *Exo* olefin hydrogens are shown using the red circle and the *endo* olefin hydrogens are the blue stars.

An attempt was made to improve M_n and $Đ$ values by manipulating t_R. With a t_R of 7.5 s, there is slight improvement of both M_n and $Đ$ compared to the retention with a t_R of 22.5 s (Table 3). Although the conversion for the shorter t_R is larger (45%) than the longer $t_{R,}$ which is not to be expected, it is a minimal variation in percent conversion and can be considered a minor inconsistency to the general expectation that long t_R would lead to higher conversion. Lastly, GPC traces were monomodal, but wide as reflected by the $Đ$ values (Figure S22 and S23).

Table 3. Endo/exo **5** at varying residence times

t_R* (s)	Conv.[a] (%)	$M_{n(theor.)}$ Da	M_n[b] Da	$Đ$
22.5	40	34 547	11 000	1.67
7.5	45	34 547	22 000	1.57

*Conditions: **M:I** = 227:1, $[\mathbf{M}]_0$= 0.38 M, $[\mathbf{I}]_0$= 0.0017 M, tubular path length =92 cm, room temperature. [a]Determined by ^{1}H NMR. [b]Determined by GPC.

3.3 Flow ROMP homopolymerization study

Utilizing the optimized reaction conditions determined for **4**, various other flow homopolymerization reactions were performed on different functionalized norbornene derived monomers at room temperature. Note the 22.5 s t_R. Polymerizing the *exo* **5** afforded product polymer in high conversion with moderate control of molecular weight and dispersity (Table 4, entry 1). Protected alcohol **6**, a sterically functionalized norbornene derivative, was also successfully polymerized under the flow conditions with product polymer characterized as actual M_n of 54,000 Da and $Đ$ of 1.16 (Table 4, entry 2). Next, *exo* α-bromo ester **7** was polymerized successfully in good conversion with moderate control over M_n and $Đ$ (Table 4, Entry 3).

Table 4. Homopolymerizations under flow conditions with t_R = 22.5 s.

Monomer*	Conv.[a] (%)	$M_{n(theor.)}$ Da	M_n[b] Da	$Đ$
5	94	34 547	43 400	1.30
6	93	63 678	54 000	1.16
7	90	58 825	44 000	1.33
8[c]	76	48 169	52 000	1.24

*Conditions: **M:I** = 227:1, $[\mathbf{M}]_0$= 0.38 M, $[\mathbf{I}]_0$= 0.0017 M, t_R = 22.5 s, tubular path length =92 cm, room temperature. [a]Determined by ^{1}H NMR. [b]Determined by GPC. [c]t_R = 450 s.

Flow homopolymerization reactions were performed at room temperature despite cooling to 0 °C for **4** resulting in better control of the polymerization reaction because cooling monomers **5-7** resulted in lower conversions and less control over M_n and $Đ$ as shown in Table 5. For this reason, flow reactions were performed at room temperature to ensure more narrow distributions and M_n values closer to theoretically calculated values.

Table 5. Flow homopolymerization of norbornene derived monomers performed at 0 °C.

Monomer*	Conv.[a] (%)	$M_{n(\text{theor.})}$ Da	M_n[b] Da	$Đ$
4	89	34,547	19,400	1.65
5	87	63,678	22,100	1.77
6	70	58,825	28,800	1.61

*Conditions: **M:I** = 227:1, $[\mathbf{M}]_0$= 0.38 M, $[\mathbf{I}]_0$= 0.0017 M, t_R = 22.5 s, tubular path length =92 cm,. [a]Determined by ^{1}H NMR. [b]Determined by GPC. [c]t_R = 450 s.

GPC traces for polymerization reactions performed at 0 °C (Figure S24-S26) were monomodal, albeit lacking symmetry and sharpness to the curve, as quantitatively expressed in $Đ$ values presented in Table 5.

3.4 Homopolymerizations at shorter residence time

Due to the rudimentary experimental setup of a basic syringe pump and the pump's limited range of attainable flow rates, a flow rate of 2 mL/min was initially used for all flow homopolymerization reactions, which correlated to a t_R of 22.5 s. When a faster flow rate of 6 mL/min was tested (closer to the upper limit of performable flow rates for the dual syringe pump) equating to a t_R of 7.5 s, an improvement in M_n and $Đ$ were observed for monomers **4-7** (Table 6). The improvement in polymer characterization values is likely due to less opportunity for side reactions to occur at a shorter t_R. For instance, backbiting (Figure 34) or chain transfer (Figure 35) reactions could occur involving the alkene bonds in the polymer backbone and the ruthenium

carbene of the "living polymer chain; this can result in a wider variety of polymer chain lengths which would account in discrepancies of M_n and $Đ$ values.

Table 6. Homopolymerizations under flow conditions

Monomer*	Conv.[a] (%)	$M_{n(\text{theor.})}$ Da	M_n[b] Da	$Đ$
4	>95	21 372	36 500	1.07
5	86	34 547	34 900	1.11
6	>95	63 678	68 300	1.18
7	83	58 825	45 200	1.12

*Conditions: **M:I** = 227:1, $[\mathbf{M}]_0$= 0.38 M, $[\mathbf{I}]_0$= 0.0017 M, t_R = 7.5 s, tubular path length =92 cm, room temperature. [a]Determined by ^{1}H NMR. [b]Determined by GPC.

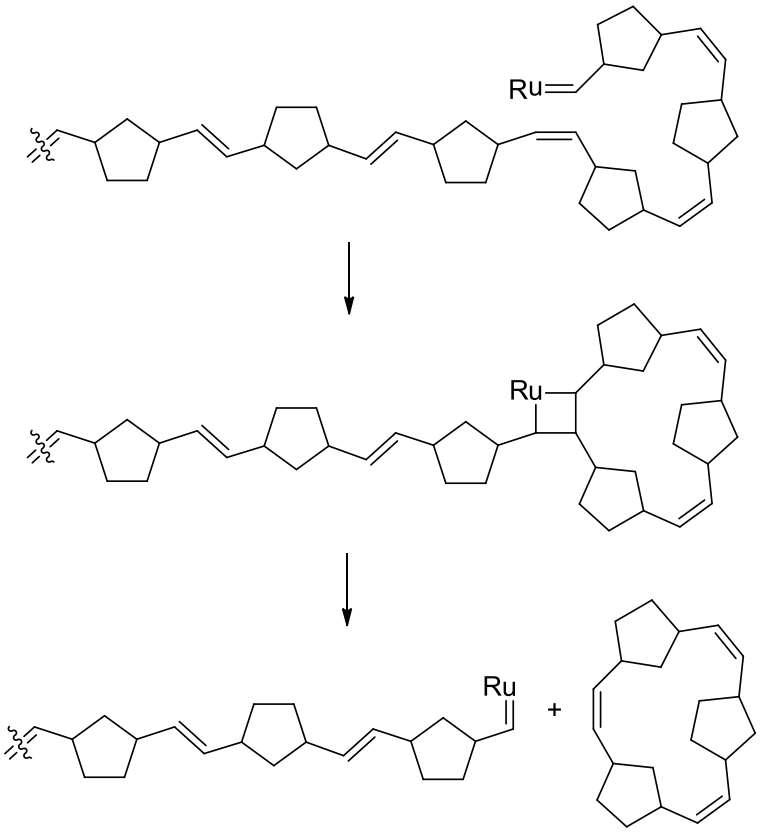

Figure 34. Backbiting side polymerization reaction.

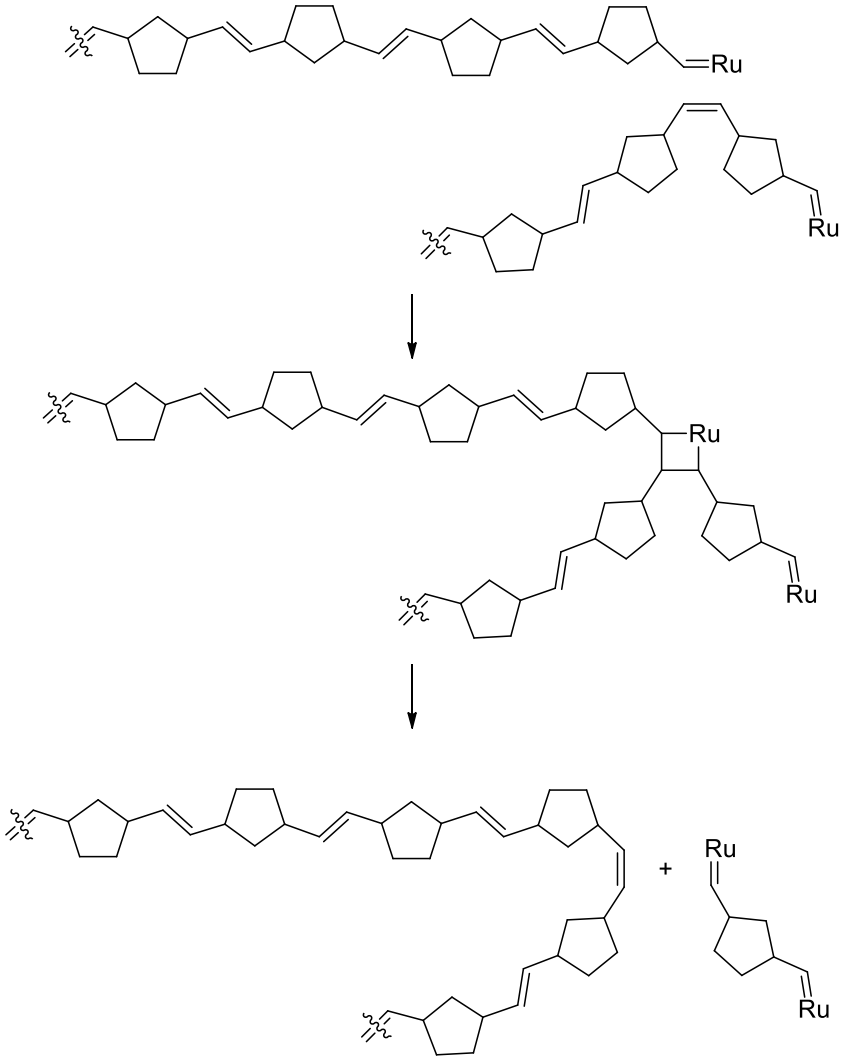

Figure 35. Chain-transfer polymerization reaction.

The GPC traces of the homopolymerization reactions carried out with a t_R = 22.5 s were monomodal, but *Đ* values were higher than expected and M_n values were not in great agreement with theoretical values. Upon shorting t_R to 7.5 s, the GPC traces remained monomodal, and *Đ* values were lower correlating to a more narrow distribution in GPC traces (Figure S27-S32). Furthermore, M_n values were more in agreement with theoretical values as can be seen in Table 6.

Another idea investigated was the influence of having non-deoxygenated solutions for the flow reactions. Using monomer **5**, a homopolymerization reaction was performed where both the monomer and initiator solutions were degassed using a freeze-pump-thaw methodology prior to being loaded into the plastic syringes. With t_R = 7.5 s, the polymer was generated in >95% conversion of monomer to polymer, but the experimental M_n value was determined by GPC to be only 26,640 Da with $Đ$ equal to 1.45. The reason why polymer characterization values were worse compared to performing the reaction without the degassing step (Table 6, Entry 2) is likely due to the initiator being dissolved in the DCM for a longer time, allowing for more initiator decomposition prior to beginning the flow reaction. This would explain the larger $Đ$ value since the degree of control over the polymerization reaction using the degassed solutions was less because a greater distribution of polymers were generated. Better results are shown when the initiator is dissolved and loaded into the syringe immediately before beginning the flow reaction to allow for minimal decomposition of initiator.

3.5 Monomer scope

Oxanorbornene **8** was polymerized, but with an astonishingly low 20% conversion from monomer to polymer when subject to the outlined generalized homopolymerization procedure. Coordination of the oxanorbornene oxygen to the Ru center of the **3** initiator likely retarded polymerization rates as has been previously observed.[47] To remedy the low conversion that was resultant of the slower polymerization rate, the t_R was increased to 450 s (flow rate of 0.1 mL/min) (Figure 36). Lamentably, **19** was generated in 76% conversion of monomer to polymer, notably lower than the conversions of **4**-**7**. However, adequate control over the polymerization was

observed with M_n and $Đ$ values of 52,000 Da and 1.24 respectively for **19**. The GPC trace showed a leading bump in the curve, likely due to the generation of larger polymer chains through side reactions such as chain transfer and back-biting reactions. Also, the curve does not return back to baseline immediately, further corroborating the possibility that some smaller chains were generated through side reactions as well (Figure S15).

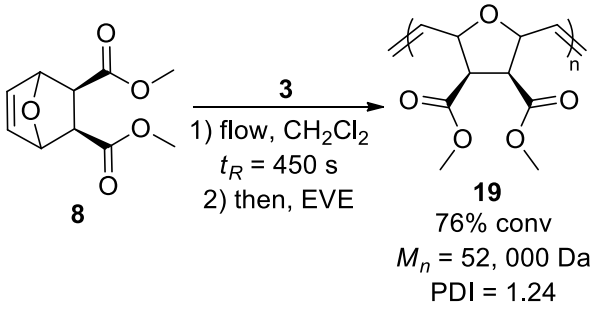

Figure 36. Homopolymerization of 8 with prolonged residence time of 450 s.

Going into this research, there was hope to successfully be able to polymerize under flow conditions non-norbornene derived monomers (Figure 37). When cyclooctene (**20**) and cyclooctadiene (**21**), with ring strain values of 8.7 and 13.3 kcal/mol respectively, were polymerized under general flow homopolymerization results (t_R = 22.5 s), a black viscous oil formed which was incapable of being analyzed by GPC due to the inability to precipitate and isolate the polymer. Also**, 20** and **21** were polymerized in lower conversion values of 26% and 66.8% respectively. Higher yield could likely be obtained by prolonging t_R, but no comparable analysis of the polymer can be made since purification cannot be done on the viscous oil.

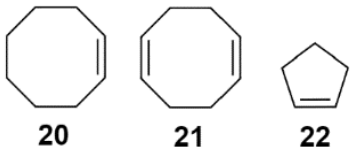

Figure 37. Non-norbornene derived monomers.

Cyclopentene (**22**) was incapable of being isolated in any significant yield at room temperature under flow conditions, likely due to its much lower ring strain value of 6.2 kcal/mol. A recent study utilized **22** as monomer for variable temperature ROMP.[48] At room temperature, the ring strain of **22** is not large enough to act as a driving force for ROMP, but at colder temperatures, ROMP can more easily be achieved. Performing ROMP under the general homopolymerization procedure outline using **22** as monomer yielded apparent high percent conversion values of >95 %, but very low percent yields of polymer after washing with methanol. It is most probably that since **22** has a boiling point of 44 °C, any monomer not polymerized was removed by vacuum prior to obtaining the crude ^{1}H NMR sample utilized to determine percent conversion of monomer to polymer. Polymerizing at 0 °C under flow conditions was ruled out due to the inability to accurately calculate percent conversion and yield with the outlined procedure since polymer was oily and not able to be precipitated in methanol.

Due to the observation of the *exo* isomer being selectively polymerized in flow, di-substituted monomers were investigated subject to the general homopolymerization procedure. Monomer **9** was polymerized to generate **23** in 92.6% conversion. However, a low control over the ROMP was evident by its actual M_n value of 12,700 Da, very low in comparison to its theoretical M_n value of 47,722 Da, as well as its high $Đ$ value of 2.20. (Figure 38). Subject to the general flow homopolymerization procedure, zero polymerization was observed in the crude ^{1}H NMR of **10** to generate **24** (Figure 39).

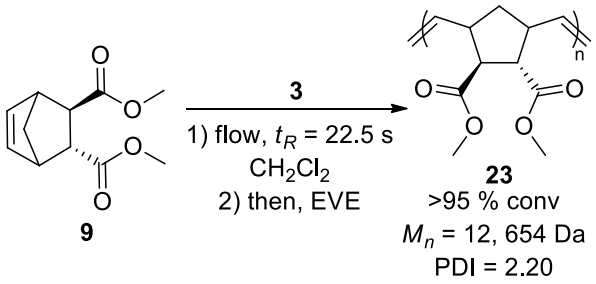

Figure 38. Homopolymerization flow reaction of **9**.

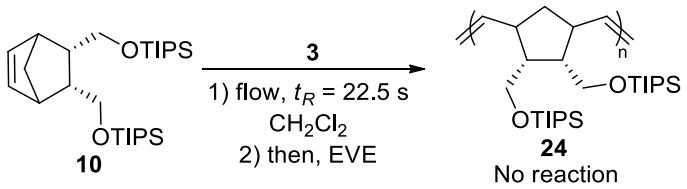

Figure 39. Homopolymerization flow reaction of **10**.

3.6 ROMP in flow "livingness" study

Theoretically, the [M]:[I] ratio dictates the number of repeating units in a generated polymer chain for a living polymerization reaction. The degree of control over a living polymerization reaction can be experimentally determined by plotting experimental M_n values as a function of [M]:[I] ratio. As the [M]:[I] ratio increases, theoretical M_n increases as well. Ideally, the $Đ$ value should remain about the same as an indicator that performing these ROMP reactions on the norbornene derived monomers is an overall well controlled polymerization reaction.

Using monomer **5**, homopolymerization flow reactions were performed at various [M]:[I] ratios. The monomer amount was consistently 1.5 mmol, and initiator amount varied. Each sample was dissolved in 4 mL of DCM prior to being pumped through with t_R = 7.5 s. The flow ROMP reactions performed are a living polymerization reaction, therefore the propagation step continues until all monomer is reacted and the polymer chain has an active termination site on the omega end of the polymer chain, or until the reaction is quenched rendering the active site on the polymer chain inactive. Ethyl vinyl

ether was used as a quenching agent for the flow polymerization reactions in this study. Through reaction with ethyl vinyl ether, the active ruthenium-carbon double bond is substituted to an inactive species containing a -CH_2 at the end of the polymer chain.

As seen in table 8 and Figure 40, M_n increases directly proportionally in relation to M:I ratio and all actual M_n values are within plus or minus 5000 Da of theoretical M_n. The R^2 of the linear regression line for the experimental data equals 0.9856, meaning the regression fit the data well. The trend observed supports the claim that performing ROMP reactions under flow conditions does not adversely affect the degree of polymerization of the reaction compared to batch. Furthermore, $Đ$ values ranges from 1.236-1.245 (Table 8), and the graph plotting $Đ$ against M:I ratios yields a line of slope approximately equal to 0 (Figure 41). The slope value can be approximated to zero to support the claim that there are no significant variation in the $Đ$, or control over polymerization for the ROMP reactions performed under flow conditions.

Table 7. GPC results for homopolymerizations of **5** at different M:I ratios.

M:I* (X:1)	$[\mathbf{I}]_0$ M	$M_{n(\text{theor.})}$ Da	$M_n{}^a$ Da	$Đ^a$
127	0.002675	19 328	19 077	1.238
227	0.001650	34 549	41 021	1.242
327	0.001163	49 766	51 970	1.239
427	0.000810	64 985	60 947	1.236
527	0.000608	80 204	75 608	1.245

*$[\mathbf{M}]_0$=0.375 M, tubular path length =92 cm, t_R = 45 s, room temperature. [a]Determined by GPC.

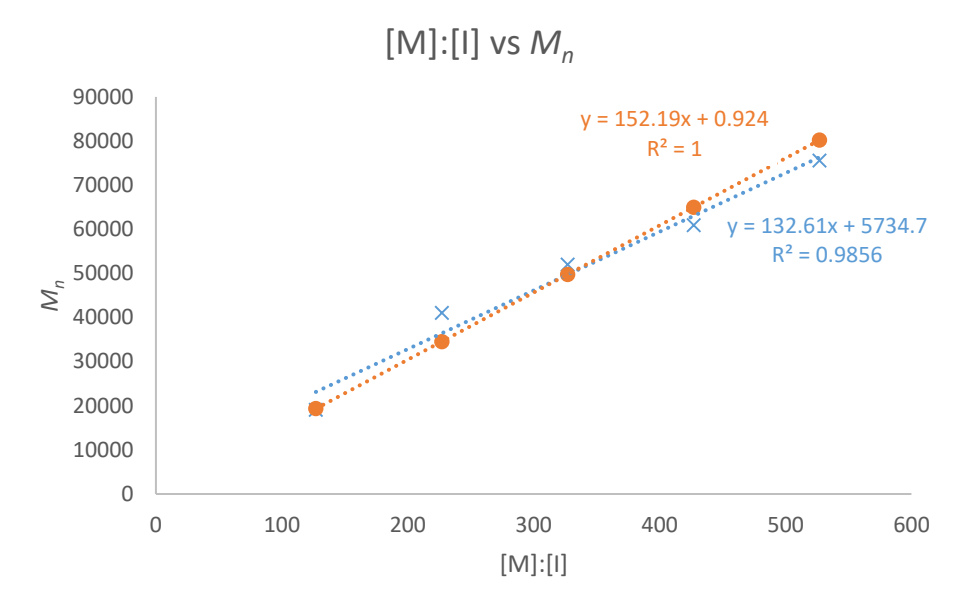

Figure 40. Graph plotting Mn values dependent on the various [M]:[I] ratios. Red circles are theoretical data points, and blue crosses are experimental data points.

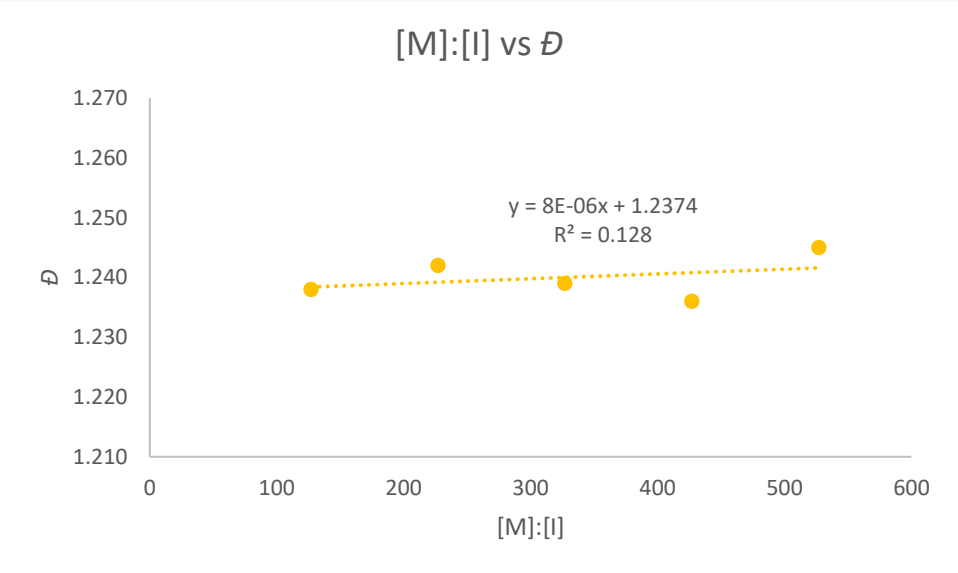

Figure 41. Graph plotting *Đ* as a function of [M]:[I] ratios.

3.7 Block copolymerizations

Under most circumstances, ROMP can be considered a living polymerization reaction, and consequently block copolymers can be generated. The flow experimental set up used to generate the homopolymers was successfully adapted by installing a

second T-mixer junction, syringe and syringe pump to facilitate the sequential second monomer addition. To demonstrate proficiency of utilizing the flow apparatus to generate block copolymers, polymers consisting of two monomers were generated. Preparing the first block was identical to that described for the homopolymerization process utilizing the dual syringe pump. After the 22.5 s t_R in the first tubular reactor, the resulting reaction solution was introduced to the second T-mixer at a rate of 2 mL/min. The second inlet portion of the T-mixer was attached to the monosyringe pump which held a syringe containing a DCM solution (0.38 M) of the second monomer (M2; **5**, **6**, or **7**). After the second 22.5 s t_R in the second tubular reactor, the block copolymer was quenched with ethyl vinyl ether.

Table 8. Block copolymerizations under flow conditions

M2*	Conv.[a] (%)	$M_{n(\text{theor.})}$ Da	M_n[b] Da	$Đ$
5	>95	24 634	35 600	1.21
6	>95	37 467	44 500	1.25
7	>95	35 329	43 600	1.27

*Conditions: **4:M2:I** = 100:100:1, $[\mathbf{4}]_0 = [\mathbf{4}]_0$ = 0.33 M, $[\mathbf{I}]_0$= 0.0033 M, reactor 1 t_R = 22.5 s, reactor 2 t_R = 22.5 s, total t_R = 45 s, tubular path length =92 cm for each reactor, room temperature. [a]With respect to both monomers, determined by ^{1}H NMR. [b]Determined by GPC.

^{1}H NMR analysis indicated apparent complete conversion for each block copolymer (Table 3). For instance, the block copolymer comprised of **4** and **5** provided **24** in 95% conversion. GPC analysis indicated M_n and $Đ$ values of 35,600 Da and 1.21, respectively (Table 3, Entry 1) (Figure 42).

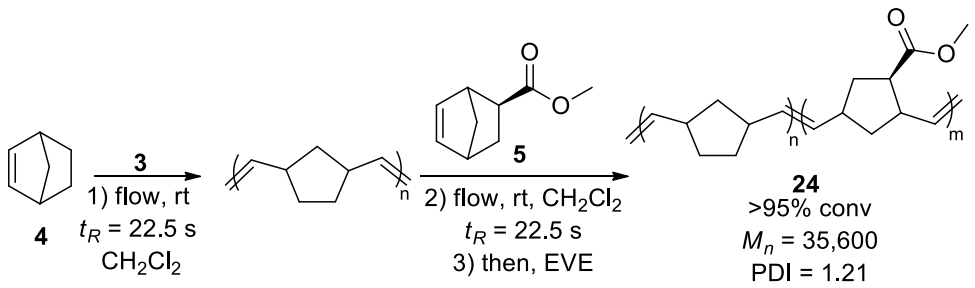

Figure 42. Block copolymerization reaction of **4** and **5**.

Seeing as the generated block copolymers consisted of two blocks of monomers with a ratio of 100:100:1 for its **4**:M2:I ratio, a homopolymer consisting of only **4** polymerized with a [M]:[I] ratio of 100:1 was generated and analyzed by GPC (Figure S33) to further corroborate the chain extension with the introduction of M2. Block copolymers of **4** with **6** and **7** were also prepared and analyzed (Table 3, entries 2, and 3, respectively). GPC analysis shows a clear shift from lower to higher molecular weights, indicating successful chain extension (Figure S34-35). Since GPC is a method of size exclusion chromatography, the larger the components that make up the sample, the shorter amount of time the sample resides within the column of the GPC, so it eludes faster and is detected at a shorter residence time. A sample of smaller molecular weight can more easily partition in and out of the porous material of the column; this means the column retains the sample longer and delays it being detected.

3.8 Thio-bromo "click" reactions

The major motivation to adapt typical batch reaction procedures for performing post-polymerization modifications to continuous flow were to cut down on the amount of materials and solvent needed to obtain the modified polymer chain. The interest was to carry out the polymerization, followed inline by the modification, without the need to stop and purify the initially polymerized starting material for the modification.

The procedure for the generation of block copolymerizations was adapted to accommodate the requirements of completing a thio-bromo click reaction. The first requirement was ensuring a sufficiently long t_R elapsed to allow complete conversion of monomer **7** to polymer within the first segment of reaction tubing, and subsequently a sufficiently long t_R for the post polymerization reaction to go to completion within the second segment of reaction tubing. Furthermore, instead of the second syringe in the monosyringe pump utilized for the block copolymerizations containing a second monomer, it was instead filled with a solution of thiol (**15**,**16**, or **17**) and triethylamine; it was possible to perform the post-polymerization modification inline. Another notable difference was the necessity of using THF instead of the DCM as solvent due to the insolubility of the salt formed between the thiol and base in syringe 2. The presence of THF meant it took a longer time to completely remove all solvent from the polymerization reaction post quenching, but before ^{1}H NMR analysis.

Nonetheless, the three post-polymerization thio-bromo click reactions worked and indicated >95% polymerization of **7** and substitution of bromine by thiol functionality. Furthermore, M_n were across the board lower than anticipated by at least 20,000 Da and $Đ$ values were within an acceptable range of 1.21-1.22 in magnitude (Table 7) (Figure S36).

Table 9. Homopolymerization of 7 and click modification under flow conditions

Thiol*	Conv.[a] (%)	$M_{n(theor.)}$ Da	M_n[b] Da	$Đ$
15	>95	65 403	43 200	1.21
16	>95	68 583	48 100	1.22
17	>95	67 738	40 000	1.21

*Conditions: **7:**thiol:Net_3:**I** = 227:681:681:1, $[\mathbf{7}]_0$= 0.38 M, $[thiol]_0$ = 2.25 M, $[\mathbf{I}]_0$= 0.00317 M, reactor 1 t_R = 22.5 s, reactor 2 t_R = 22.5 s, total t_R = 45 s, tubular path length =92 cm for each reactor, room temperature. [a]With respect to both ROMP and click reaction, determined by ^{1}H NMR. [b]Determined by GPC.

To further corroborate the ability to perform these thio-bromo click reactions in flow, an additional control reaction was performed where bromo ester **7** was polymerized in flow utilizing the homopolymerization methodology to generate **25**, quenched with ethyl vinyl ether, isolated and lastly purified. The product was then subjected to a click reaction in flow where one syringe contained **25** dissolved in DCM, and the other syringe of the dual syringe pump contained the **16**/triethylamine/THF solution to generate polymer **26** (Figure 43).

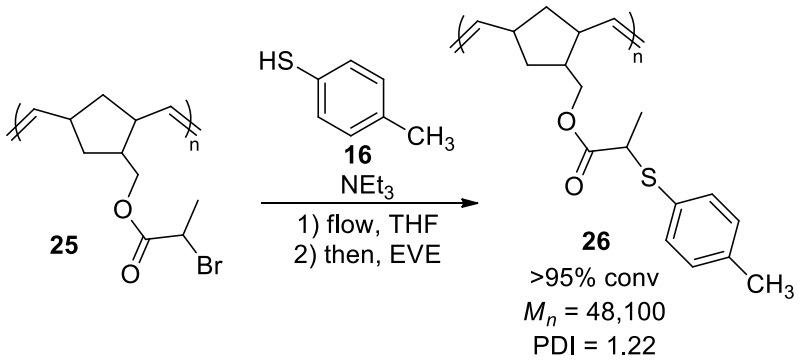

Figure 43. Control post polymerization thio-bromo click reaction.

CHAPTER III

Conclusion

Homopolymers and block copolymers were synthesized in flow using norbornene derived monomers with moderate control over molecular weight and *Đ*. Polymerizations followed inline by post-polymerization thio-bromo "click" modifications were successfully performed with >95 % conversion of starting polymer functionality to desired functionality. Upon optimization of reaction conditions for homopolymerizations in flow utilizing initiator **3** with the various norbornene derivatives, it was simple to expand the experimental setup and adapt it to accommodate both block copolymerizations and post-polymerization modifications in flow by addition of a second reactor loop and syringe pump.

The monomer scope success was limited to norbornene derived monomers because the ring strain of norbornene proved large enough to readily polymerize in flow; other monomers did not polymerize well under the outlined procedures of this study. For instance, the oxanorbornene derivative (**8**) required a significantly longer R_t to obtain a high conversion of monomer to polymer likely due to the oxygen in the norbornene bridge chelating to the ruthenium center of **3** retarding the rate of polymerization. Monocyclic monomers such as cyclopentene, cyclooctene and cyclooctadiene did not polymerize well in flow due to their much lower ring strain compared to norbornene. Disubstituted norbornene monomer derivatives were problematic as well likely due to steric effects preventing ROMP from occurring at the alkene bond in the norbornene ring.

All three block copolymerizations distinctly support successful chain extension by GPC analysis where the block copolymer trace shifted to a shorter retention time and

remained monomodal. Since the polymer sample eluted sooner than the homopolymer of the first block of **1** only, it signified larger molecular weight supporting chain extension. Furthermore, the GPC traces remained monomodal for the blockcopolymer showing chain extension and not just synthesis of two separate homopolymers.

Future work on performing ROMP under flow conditions can be expanded to include a larger monomer scope than what was explored by this study. Optimization of each monomer subset can be explored in a more exhaustive effort to perform ROMP on other monomers than norbornene derived monomers in flow. Also, a follow-up to this study could include analysis of how changing experimental parameters such as feed ratio, concentration and flow rate can affect molecular weight and $Đ$.

REFERENCE

(1) Geacintov, C.; Smid, J.; Szwarc, M. Kinetics of Anionic Polymerization of Styrene in Tetrahydrofuran. *J. Am. Chem. Soc.* **1962**, *84* (13), 2508–2514.

(2) Corrigan, N.; Almasri, A.; Taillades, W.; Xu, J.; Boyer, C. Controlling Molecular Weight Distributions through Photoinduced Flow Polymerization. *Macromolecules* **2017**, *50* (21), 8438–8448.

(3) Tonhauser, C.; Natalello, A.; Löwe, H.; Frey, H. Microflow Technology in Polymer Synthesis. *Macromolecules* **2012**, *45* (24), 9551–9570.

(4) Lévesque, F.; Rogus, N. J.; Spencer, G.; Grigorov, P.; McMullen, J. P.; Thaisrivongs, D. A.; Davies, I. W.; Naber, J. R. Advancing Flow Chemistry Portability: A Simplified Approach to Scaling Up Flow Chemistry. *Org. Process Res. Dev.* **2018**, *22* (8), 1015–1021.

(5) Ramsey, B. L.; Pearson, R. M.; Beck, L. R.; Miyake, G. M. Photoinduced Organocatalyzed Atom Transfer Radical Polymerization Using Continuous Flow. *Macromolecules* **2017**, *50* (7), 2668–2674.

(6) Zaquen, N.; Kadir, A. M. N. B. P. H. A.; Iasa, A.; Corrigan, N.; Junkers, T.; Zetterlund, P. B.; Boyer, C. Rapid Oxygen Tolerant Aqueous RAFT Photopolymerization in Continuous Flow Reactors. *Macromolecules* **2019**, *52* (4), 1609–1619.

(7) Walsh, D. J.; Guironnet, D.; Weitz, D. A. Macromolecules with Programmable Shape, Size, and Chemistry. *Proc. Natl. Acad. Sci.* **2019**, *116* (5), 1528–1542.

(8) Shen, X.; Gong, H.; Zhou, Y.; Zhao, Y.; Lin, J.; Chen, M. Unsymmetrical Difunctionalization of Cyclooctadiene under Continuous Flow Conditions:

Expanding the Scope of Ring Opening Metathesis Polymerization. *Chem. Sci.* **2018**, *9* (7), 1846–1853.

(9) Bandari, R.; Buchmeiser, M. R. Polymeric Monolith Supported Pt-Nanoparticles as Ligand-Free Catalysts for Olefin Hydrosilylation under Batch and Continuous Conditions. *Catal. Sci. Technol.* **2012**, *2* (1), 220–226.

(10) Grubbs, R. B.; Grubbs, R. H. 50th Anniversary Perspective: Living Polymerization—Emphasizing the Molecule in Macromolecules. *Macromolecules* **2017**, *50* (18), 6979–6997.

(11) Caire da Silva, L.; Rojas, G.; Schulz, M. D.; Wagener, K. B. Acyclic Diene Metathesis Polymerization: History, Methods and Applications. *Prog. Polym. Sci.* **2016**, *69* (2017), 79–107.

(12) Topolovčan, N.; Panov, I.; Kotora, M. Synthesis of 1,2-Disubstituted Cyclopentadienes from Alkynes Using a Catalytic Haloallylation/Cross-Coupling/Metathesis Relay. *Org. Lett.* **2016**, *18* (15), 3634–3637.

(13) Voigtritter, K.; Ghorai, S.; Lipshutz, B. H. Rate Enhanced Olefin Cross-Metathesis Reactions: The Copper Iodide Effect. *J. Org. Chem.* **2011**, *76* (11), 4697–4702.

(14) Lerum, M. F. Z.; Chen, W. Surface-Initiated Ring-Opening Metathesis Polymerization in the Vapor Phase: An Efficient Method for Grafting Cyclic Olefins with Low Strain Energies. *Langmuir* **2011**, *27* (9), 5403–5409.

(15) Adekunle, O.; Tanner, S.; Binder, W. H. Synthesis and Crossover Reaction of TEMPO Containing Block Copolymer via ROMP. *Beilstein J. Org. Chem.* **2010**, *6* (59), 1–11.

(16) Liu, F.; Xu, N.; Ling, L.; Hu, J.; Zhang, H. Regio-and Stereoselective Ring-

Opening Metathesis Polymerization of 3-Ferrocenyl Substituted Cyclooctenes and Copolymerization with Norbornene Derivatives. *Eur. Polym. J.* **2020**, *124* (2020), 1–8.

(17) Choi, T. L.; Grubbs, R. H. Controlled Living Ring-Opening-Metathesis Polymerization by a Fast-Initiating Ruthenium Catalyst. *Angew. Chem. Int. Ed.* **2003**, *42* (15), 1743–1746.

(18) Reddy, F. N. Olefin Homologation with Titanium Methylene Compounds. *J. Am. Chem. Soc* **1978**, *100* (11), 3611–3613.

(19) SonBinh T. Nguyen, L. K. J.; Grubbs*, R. H. Ring-Opening Metathesis Polymerization (ROMP) of Norbornene by a Group VIII Carbene Complex in Protic Media. *J. Am. Chem. Soc.* **1985**, *107* (3), 737–738.

(20) Schrock, R. R.; Murdzek, J. S.; Bazan, G. C.; Robbins, J.; DiMare, M.; O'Regan, M. Synthesis of Molybdenum Imido Alkylidene Complexes and Some Reactions Involving Acyclic Olefins. *J. Am. Chem. Soc.* **1990**, *112* (6), 899.

(21) Nguyen, S. T.; Johnson, L. K.; Grubbs, R. H.; Beckman, M.; Ziller, J. W. Ring-Opening Metathesis Polymerization (ROMP) of Norbornene by a Group VIII Carbene Complex in Protic Media. *J. Am. Chem. Soc.* **1992**, *114* (92), 3974–3975.

(22) Arduengo, A. J.; Dias, H. V. R.; Harlow, R. L.; Kline, M. Electronic Stabilization of Nucleophilic Carbenes. *J. Am. Chem. Soc.* **1992**, *114* (14), 5530–5534.

(23) Scholl, M.; Ding, S.; Lee, C. W.; Grubbs, R. H. Synthesis and Activity of a New Generation of Ruthenium-Based Olefin Metathesis Catalysts Coordinated with 1,3-Dimesityl-4,5-Dihydroimidazol-2-Ylidene Ligands. *Org. Lett.* **1999**, *1* (6), 953–956.

(24) Bielawski, C. W.; Grubbs, R. H. Highly Efficient Ring-Opening Metathesis Polymerization (ROMP) Using New Ruthenium Catalysts Containing N-Heterocyclic Carbene Ligands. *Angew. Chem. Int. Ed.* **2000**, *39* (16), 2903–2906.

(25) Walsh, D. J.; Lau, S. H.; Hyatt, M. G.; Guironnet, D. Kinetic Study of Living Ring-Opening Metathesis Polymerization with Third-Generation Grubbs Catalysts. *J. Am. Chem. Soc.* **2017**, *139* (39), 13644–13647.

(26) Tomasek, J.; Schatz, J. Olefin Metathesis in Aqueous Media. *Green Chem.* **2013**, *15* (9), 2317–2338.

(27) Hein, C. D.; Liu, X. M.; Wang, D. Click Chemistry, a Powerful Tool for Pharmaceutical Sciences. *Pharm. Res.* **2008**, *25* (10), 2216–2230.

(28) Binder, W. H.; Sachsenhofer, R. 'Click' Chemistry in Polymer and Materials Science. *Macromol. Rapid Commun.* **2007**, *28* (1), 15–54.

(29) Forshaw, S.; Knighton, R. C.; Reber, J.; Parker, J. S.; Chmel, N. P.; Wills, M. A Strained Alkyne-Containing Bipyridine Reagent; Synthesis, Reactivity and Fluorescence Properties. *RSC Adv.* **2019**, *9* (62), 36154–36161.

(30) Sun, Y.; Liu, H.; Cheng, L.; Zhu, S.; Cai, C.; Yang, T.; Yang, L.; Ding, P. Thiol Michael Addition Reaction: A Facile Tool for Introducing Peptides into Polymer-Based Gene Delivery Systems. *Polym. Int.* **2018**, *67* (1), 25–31.

(31) Altintas, O.; Willenbacher, J.; Wuest, K. N. R.; Oehlenschlaeger, K. K.; Krolla-Sidenstein, P.; Gliemann, H.; Barner-Kowollik, C. A Mild and Efficient Approach to Functional Single-Chain Polymeric Nanoparticles via Photoinduced Diels–Alder Ligation. *Macromolecules* **2013**, *46* (20), 8092–8101.

(32) Rosen, B. M.; Lligadas, G.; Hahn, C.; Percec, V. Synthesis of Dendritic

Macromolecules through Divergent Iterative Thio-Bromo “Click” Chemistry and SET-LRP. *J. Polym. Sci. Part A Polym. Chem.* **2009**, *47* (15), 3940–3948.

(33) Hobbs, C. E.; Vasireddy, M. Combining ATRP and ROMP with Thio-Bromo, Copper-Catalyzed, and Strain-Promoted Click Reactions for Brush Copolymer Synthesis Starting from a Single Initiator/Monomer/Click Partner. *Macromol. Chem. Phys.* **2019**, *220* (7), 1800497–1800503.

(34) Yao, Q.; Gutierrez, D. C.; Hoang, N. H.; Kim, D.; Wang, R.; Hobbs, C.; Zhu, L. Efficient Codelivery of Paclitaxel and Curcumin by Novel Bottlebrush Copolymer-Based Micelles. *Mol. Pharm.* **2017**, *14* (7), 2378–2389.

(35) Ashok Kothapalli, V.; Shetty, M.; De Los Santos, C.; Hobbs, C. E. Thio-Bromo “Click,” Post-Polymerization Strategy for Functionalizing Ring Opening Metathesis Polymerization (ROMP)-Derived Materials. *J. Polym. Sci. Part A Polym. Chem.* **2016**, *54* (1), 179–185.

(36) Grubb, J.; Carosio, F.; Vasireddy, M.; Moncho, S.; Brothers, E. N.; Hobbs, C. E. Ring Opening Metathesis Polymerization (ROMP) and Thio-Bromo “Click” Chemistry Approach toward the Preparation of Flame-Retardant Polymers. *J. Polym. Sci. Part A Polym. Chem.* **2018**, *56* (6), 645–652.

(37) Ashlin, M.; Hobbs, C. E. Post-Polymerization Thiol Substitutions Facilitated by Mechanochemistry. *Macromol. Chem. Phys.* **2019**, *220* (21), 1900350–1900357.

(38) Njoroge, I.; Kempler, P. A.; Deng, X.; Arnold, S. T.; Jennings, G. K. Surface-Initiated Ring-Opening Metathesis Polymerization of Dicyclopentadiene from the Vapor Phase. *Langmuir* **2017**, *33* (49), 13903–13912.

(39) Radzinski, S. C.; Foster, J. C.; Matson, J. B. Preparation of Bottlebrush Polymers

via a One-Pot Ring-Opening Polymerization (ROP) and Ring-Opening Metathesis Polymerization (ROMP) Grafting-Through Strategy. *Macromol. Rapid Commun.* **2016**, *37* (7), 616–621.

(40) Kanao, M.; Otake, A.; Tsuchiya, K.; Ogino, K. Stereo-Selective Synthesis of 5-Norbornene-2-Exo-Carboxylic Acid—Rapid Isomerization and Kinetically Selective Hydrolysis. *Int. J. Org. Chem.* **2012**, *02* (01), 26–30.

(41) Sun, G.; Hentschel, J.; Guan, Z. Synthesis of "Necklace" Polymers by Chain-Walking Polymerization. *ACS Macro Lett.* **2012**, *1* (5), 585–588.

(42) Ashok Kothapalli, V.; Shetty, M.; de los Santos, C.; Hobbs, C. E. Thio-Bromo "Click," Post-Polymerization Strategy for Functionalizing Ring Opening Metathesis Polymerization (ROMP)-Derived Materials. *J. Polym. Sci. Part A Polym. Chem.* **2016**, *54* (1), 179–185.

(43) Ye, L.; Zhang, S. F.; Lin, Y. C.; Min, J. K.; Ma, L.; Tang, T. Synthesis and Characterization of Butyl Acrylate-Based Graft Polymers with Thermo-Responsive Branching Sites via the Diels-Alder Reaction of Furan/Maleimide. *Chinese J. Polym. Sci.* **2018**, *36* (9), 1011–1018.

(44) France, M. B.; Alty, L. T.; Earl, T. M. Synthesis of a 7-Oxanorbornene Monomer: A Two-Step Sequence Preparation for the Organic Laboratory. *J. Chem. Educ.* **2009**, *76* (5), 659–660.

(45) Hickey, S. M.; Ashton, T. D.; White, J. M.; Li, J.; Nation, R. L.; Yu, H. Y.; Elliott, A. G.; Butler, M. S.; Huang, J. X.; Cooper, M. A.; et al. Synthesis of Norbornane Bisether Antibiotics via Silver-Mediated Alkylation. *RSC Adv.* **2015**, *5* (36), 28582–28596.

(46) Liu, P.; Yasir, M.; Ruggi, A.; Kilbinger, A. F. M. Heterotelechelic Polymers by Ring-Opening Metathesis and Regioselective Chain Transfer. *Angew. Chem. Int. Ed.* **2018**, *57* (4), 914–917.

(47) Yang, B.; Abel, B. A.; McCormick, C. L.; Storey, R. F. Synthesis of Polyisobutylene Bottlebrush Polymers via Ring-Opening Metathesis Polymerization. *Macromolecules* **2017**, *50* (19), 7458–7467.

(48) Neary, W. J.; Kennemur, J. G. Variable Temperature ROMP: Leveraging Low Ring Strain Thermodynamics To Achieve Well-Defined Polypentenamers. *Macromolecules* **2017**, *50* (13), 4935–4941.

APPENDIX

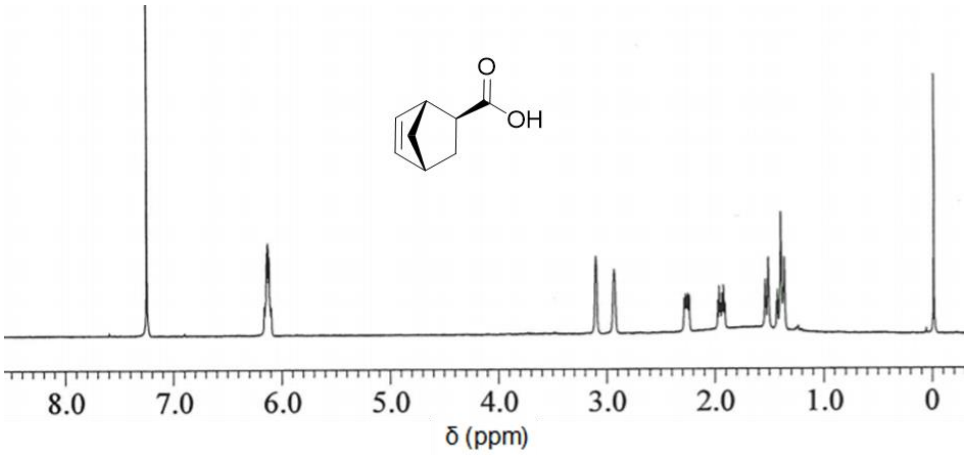

Figure S1. ^{1}H NMR spectrum of *exo*-2-norbornene-5-carboxylic acid (**11**) in $CDCl_3$

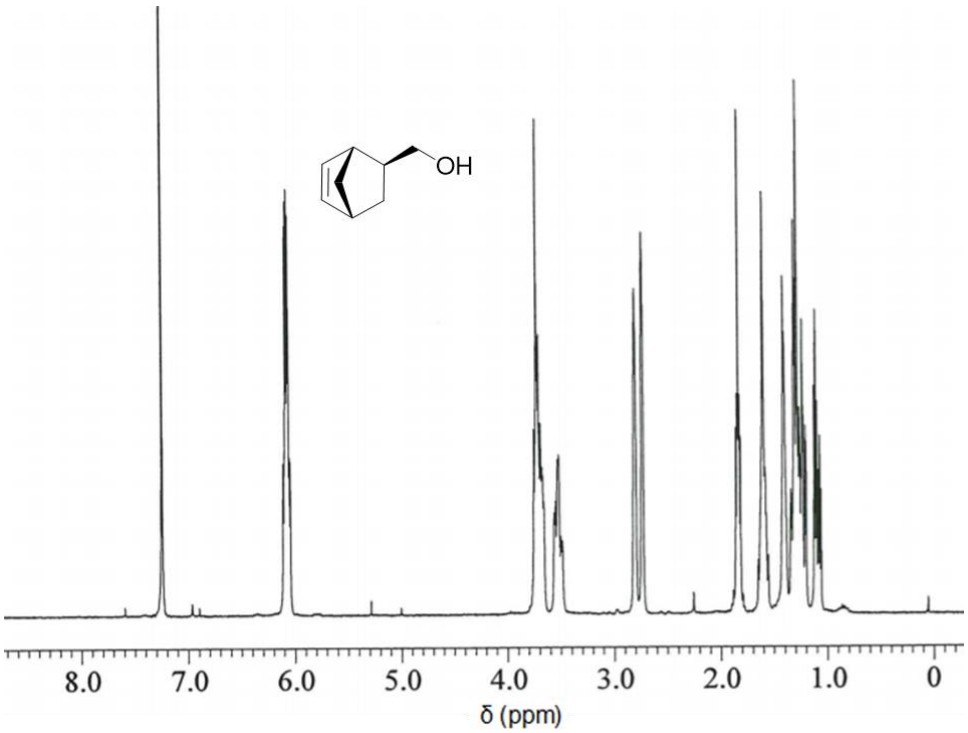

Figure S2. ^{1}H NMR spectrum of *exo*-5-norbornene-2-methanol (**12**) in $CDCl_3$

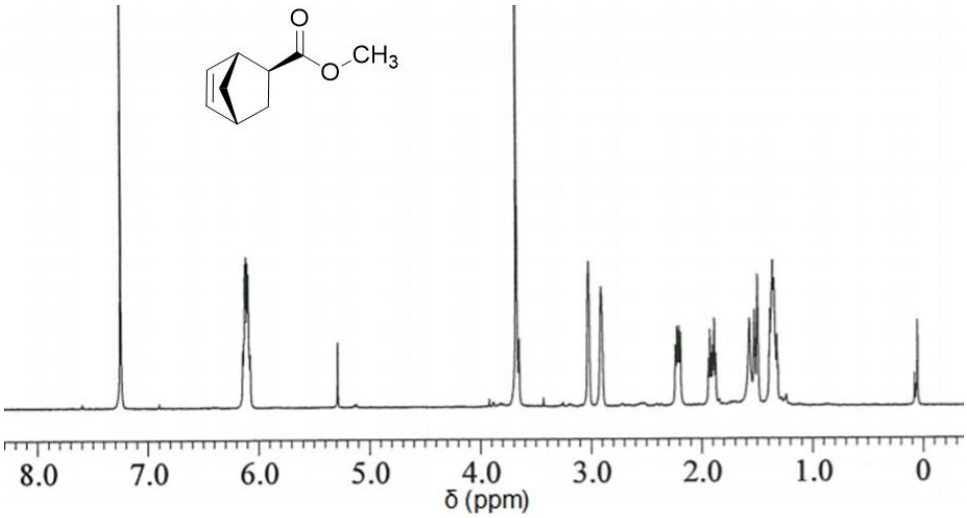

Figure S3. ^{1}H NMR spectrum of methyl *exo*-2-norbornene-5-carboxylate (**5**) in $CDCl_3$

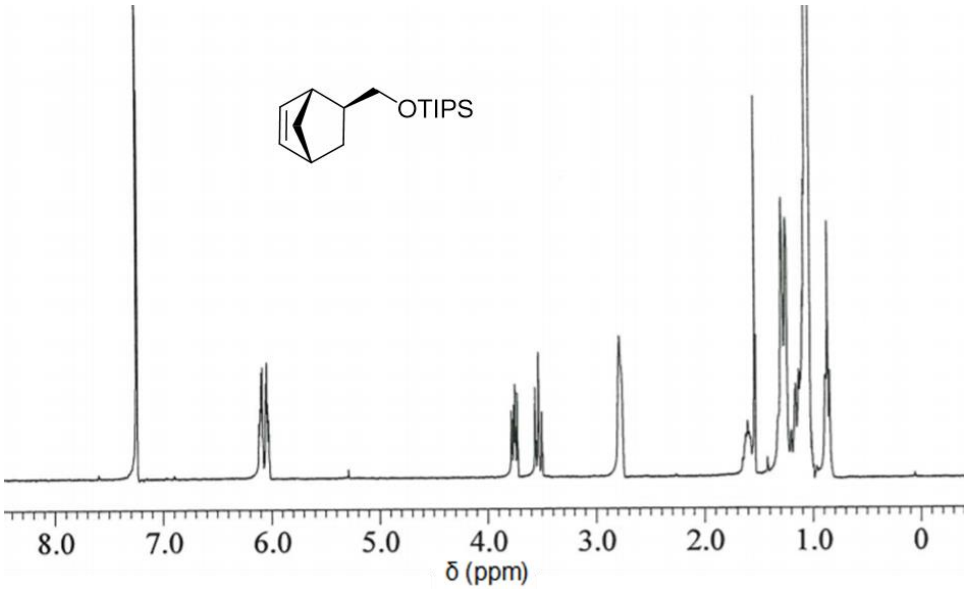

Figure S4. ^{1}H NMR spectrum of -TIPS protected *exo*-5-norbornene-2-methanol (**6**) in $CDCl_3$

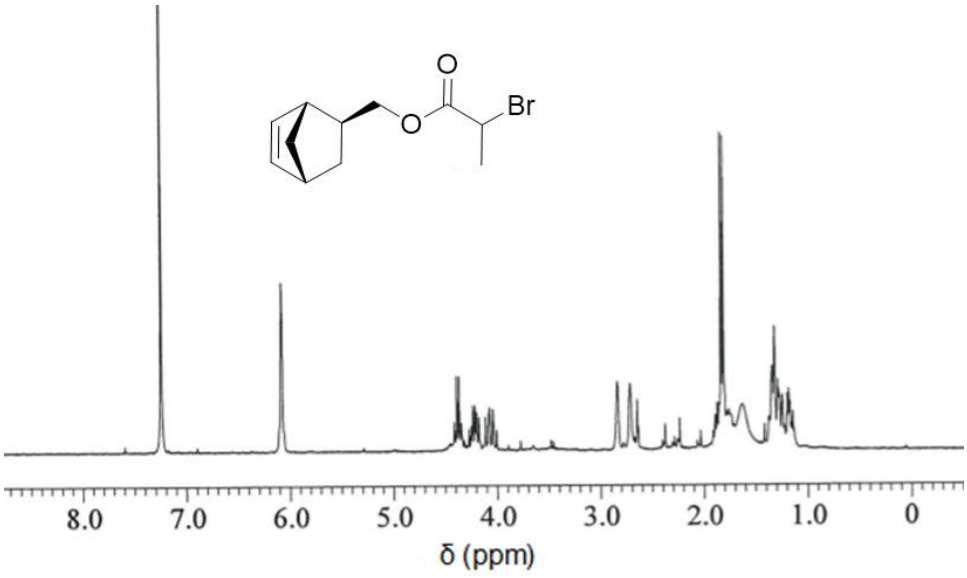

Figure S5. ^{1}H NMR spectrum of *exo*-5-norbornene-2-bromopropionate (**7**) in $CDCl_3$

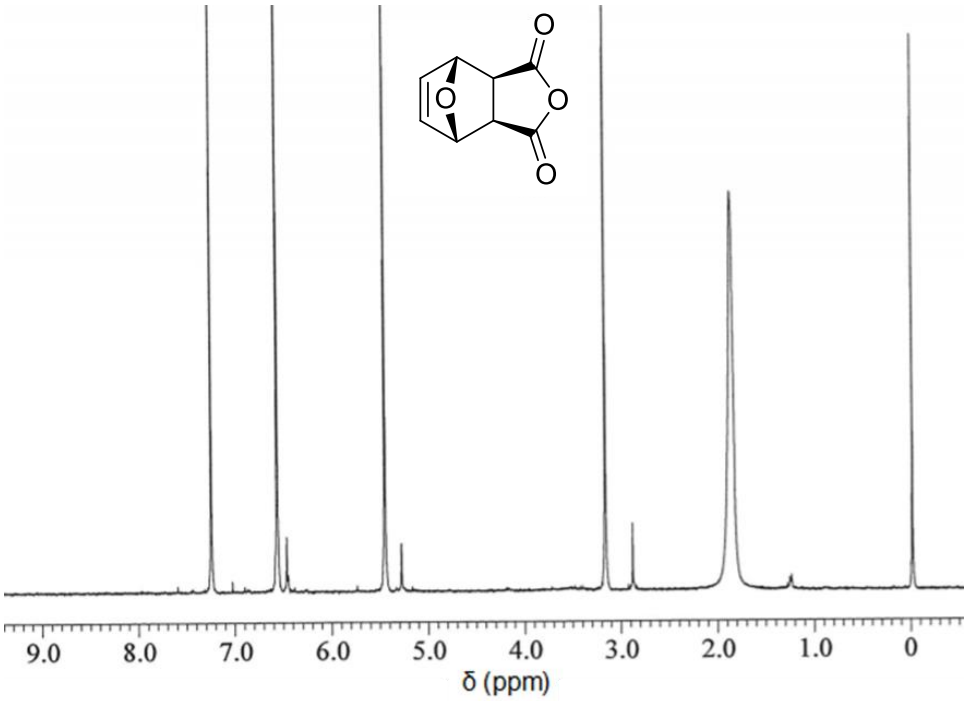

Figure S6. ^{1}H NMR spectrum of furan-maleic anhydride adduct (**13**) in $CDCl_3$

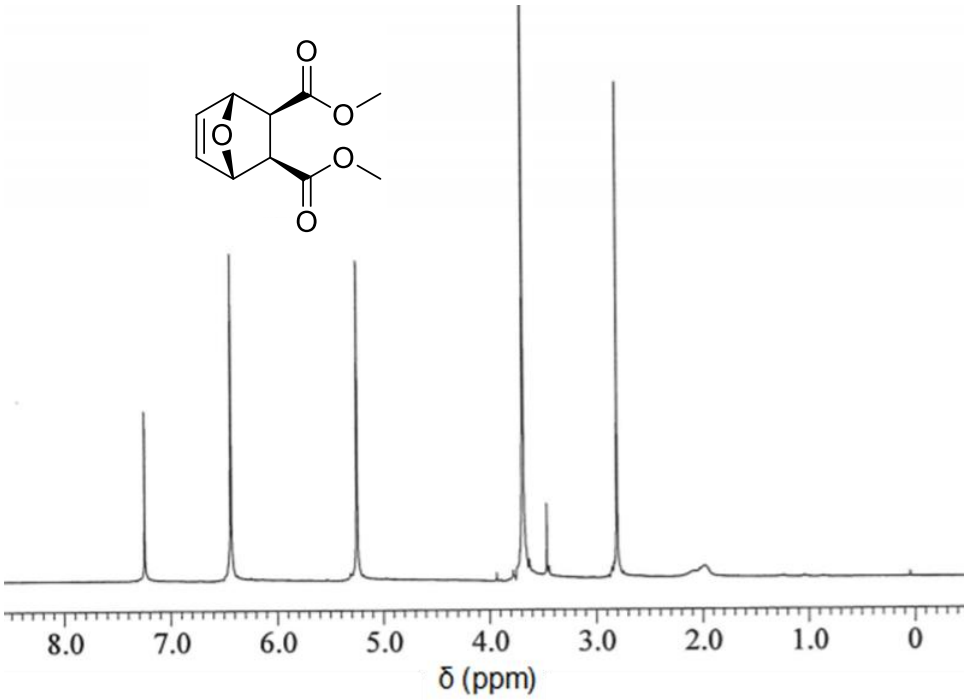

Figure S7. ^{1}H NMR spectrum of oxa-norbornene-dimethyl-2,3-dicarboxylate (**8**) in $CDCl_3$

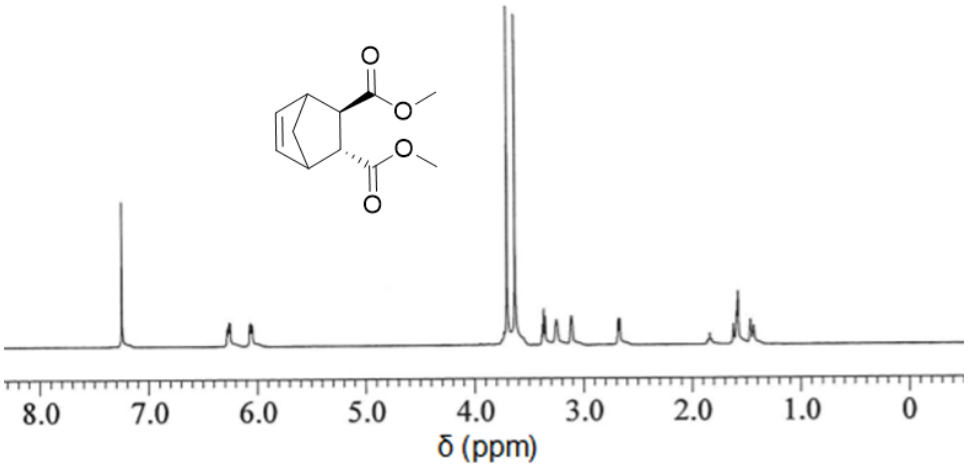

Figure S8. ^{1}H NMR spectrum of norbornene-dimethyl 2-*endo*, 3-*exo*-dicarboxylate (**9**) in $CDCl_3$

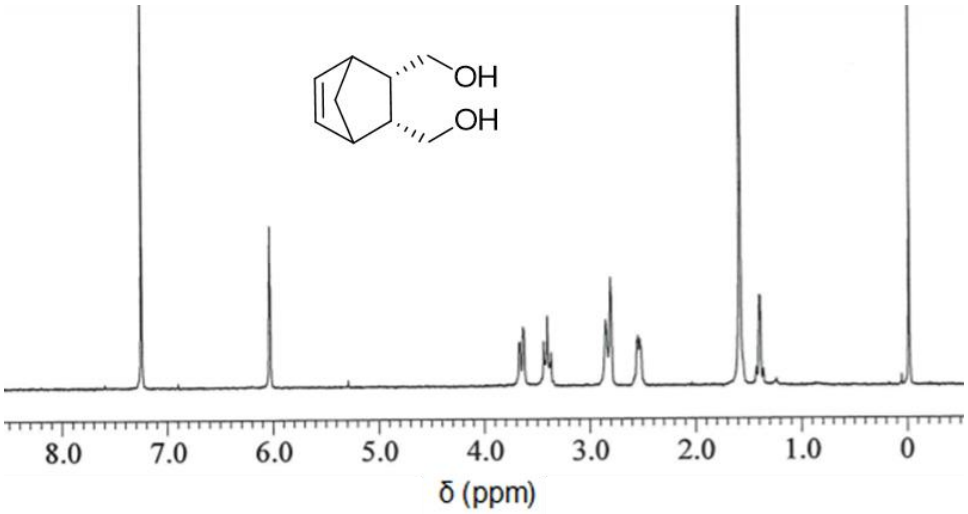

Figure S9. ^{1}H NMR spectrum of *endo*-5-norbornene-2,3-methanol (**14**) in $CDCl_3$

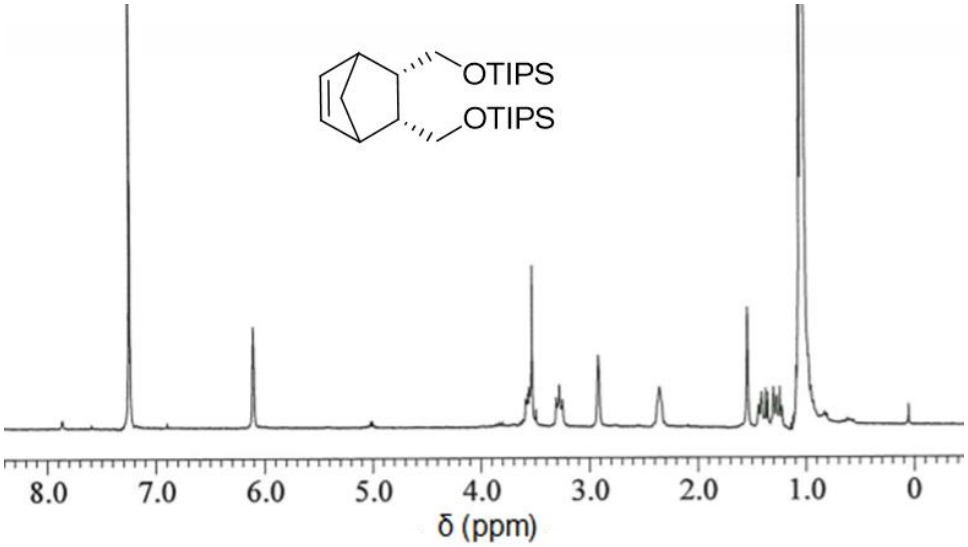

Figure S10. ^{1}H NMR spectrum of di-TIPS protected *endo*-5-norbornene-2,3-methanol (**10**) in $CDCl_3$

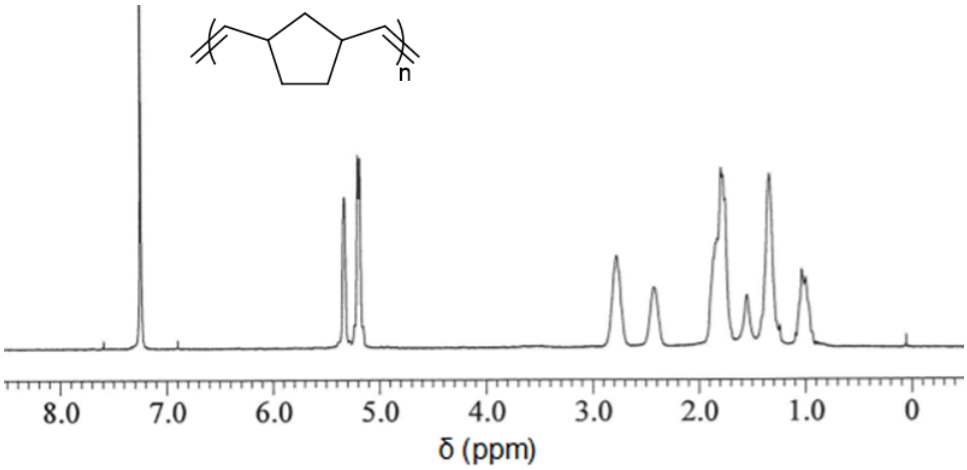

Figure S11. ^{1}H NMR spectrum of polymerized norbornene (**4**) in $CDCl_3$

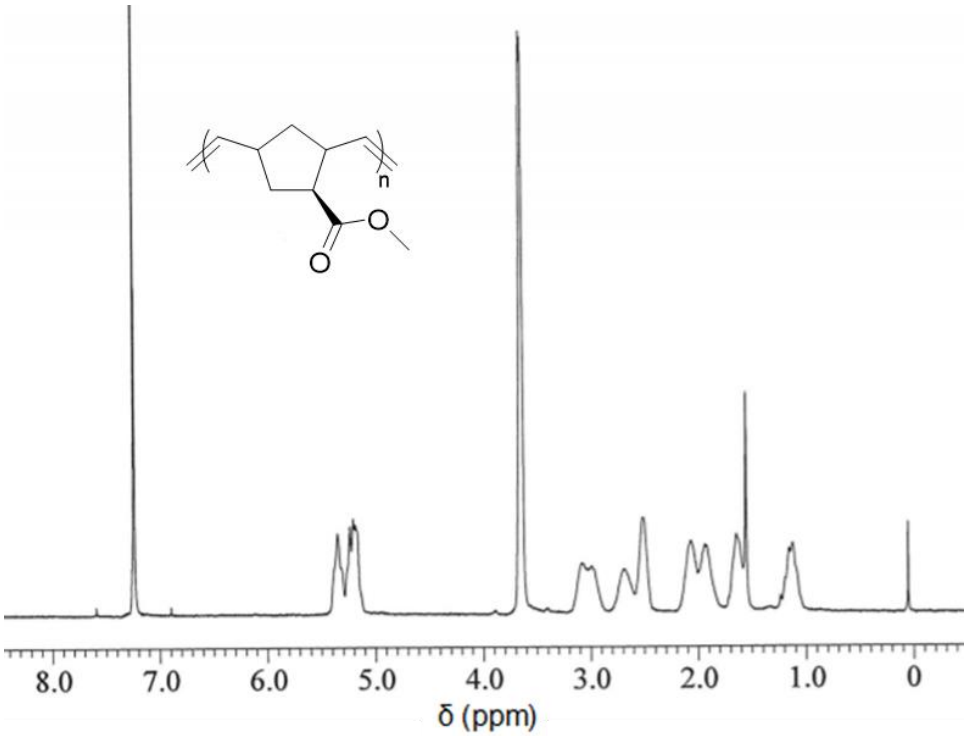

Figure S12. ^{1}H NMR spectrum of polymerized methyl *exo*-2-norbornene-5-carboxylate (**2**) in $CDCl_3$

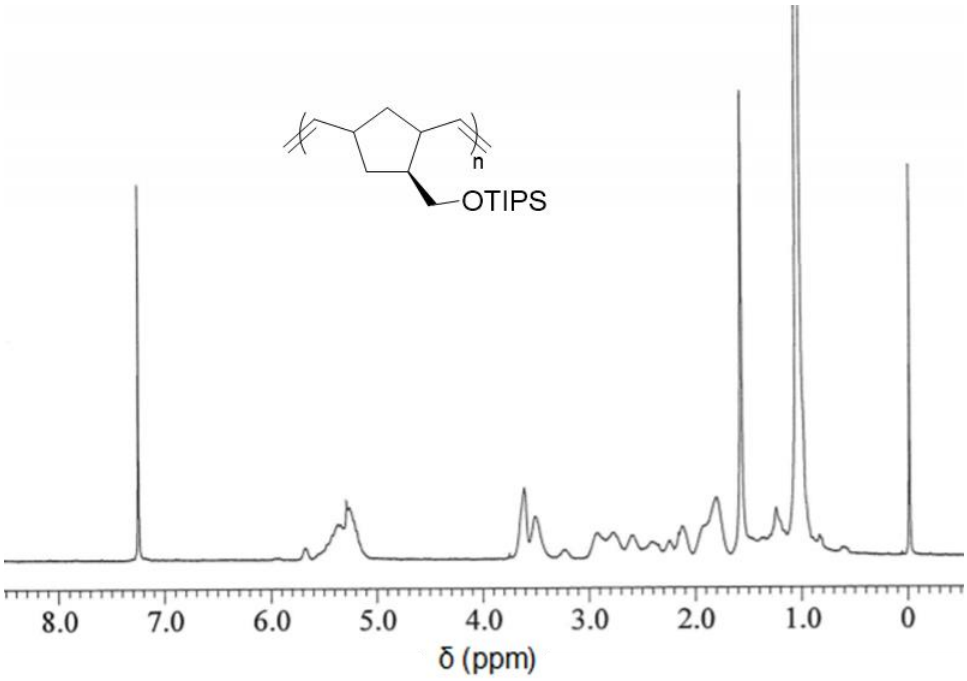

Figure S13. ^{1}H NMR spectrum of polymerized TIPS protected *exo*-5-norbornene-2-methanol (**6**) in $CDCl_3$

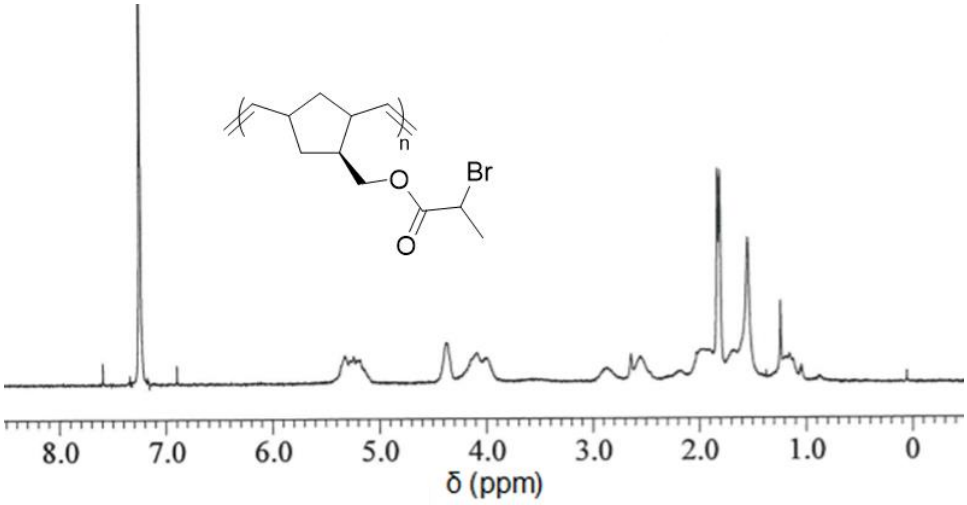

Figure S14. ^{1}H NMR spectrum of polymerized *exo*-5-norbornene-2-bromopropionate (**7**) in $CDCl_3$

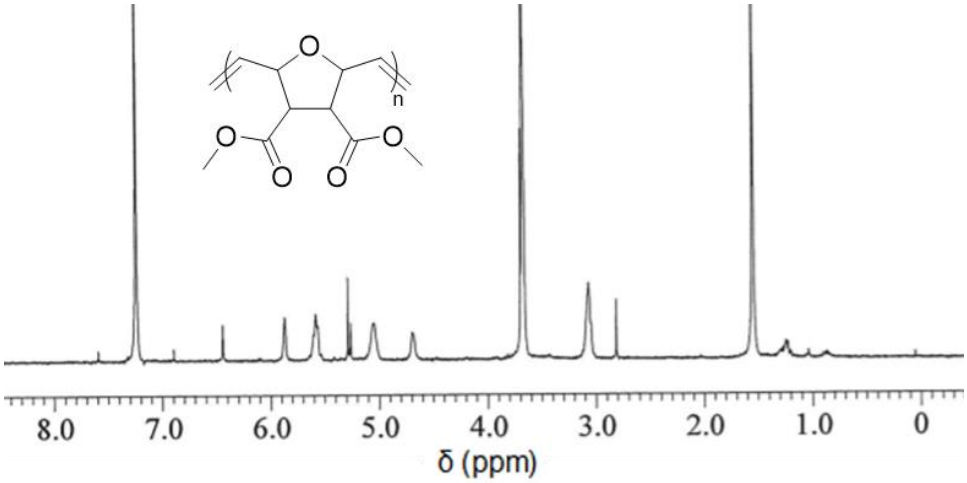

Figure S15. ^{1}H NMR spectrum of polymerized oxa-norbornene-dimethyl-2,3-dicarboxylate (**8**) in $CDCl_3$

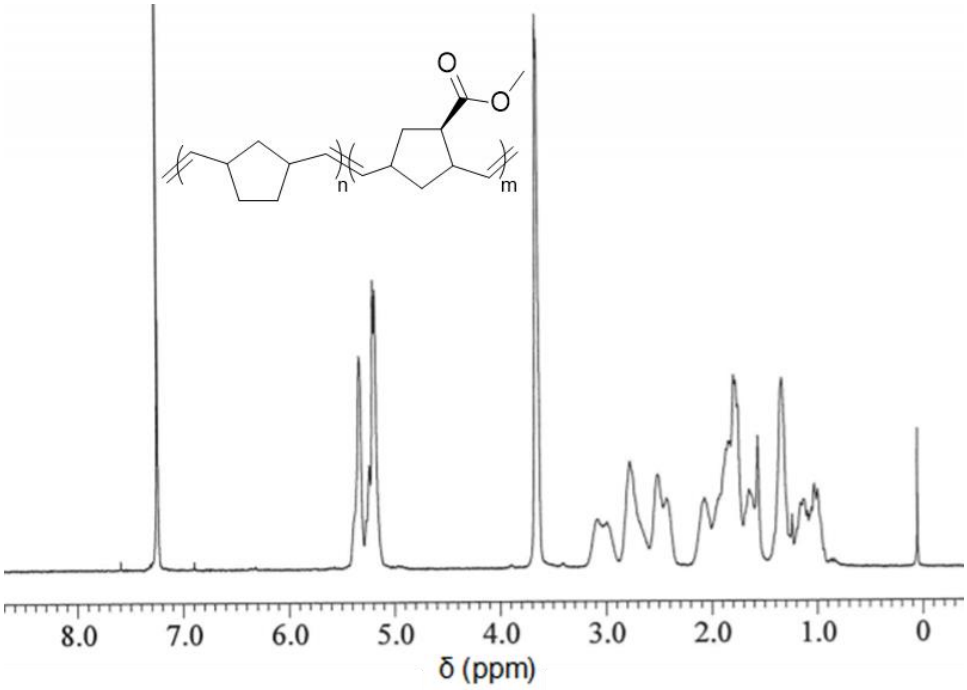

Figure S16. ^{1}H NMR spectrum of block copolymer (**4**) and (**5**) in $CDCl_3$

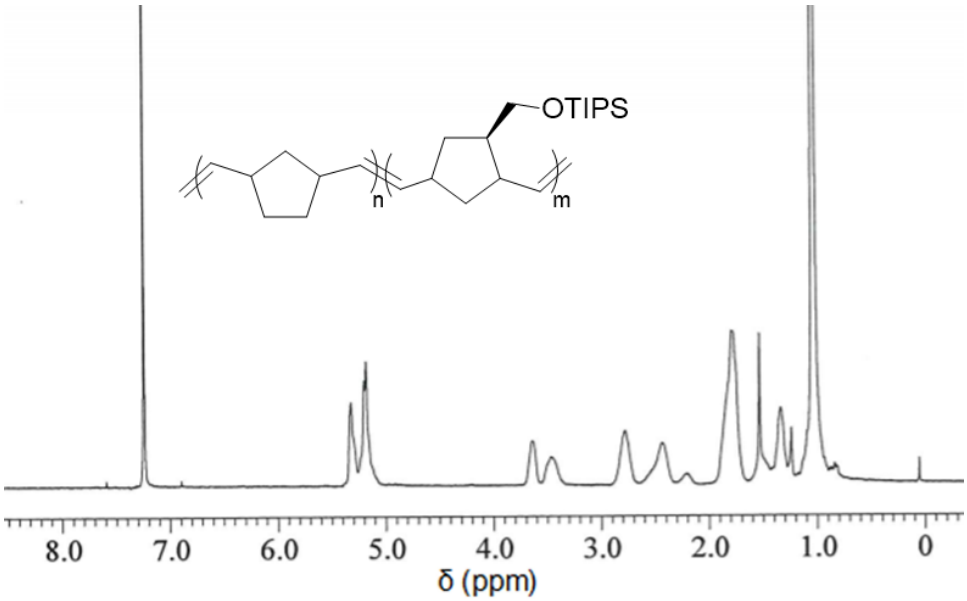

Figure S17. ^{1}H NMR spectrum of block copolymer (**4**) and (**6**) in $CDCl_3$

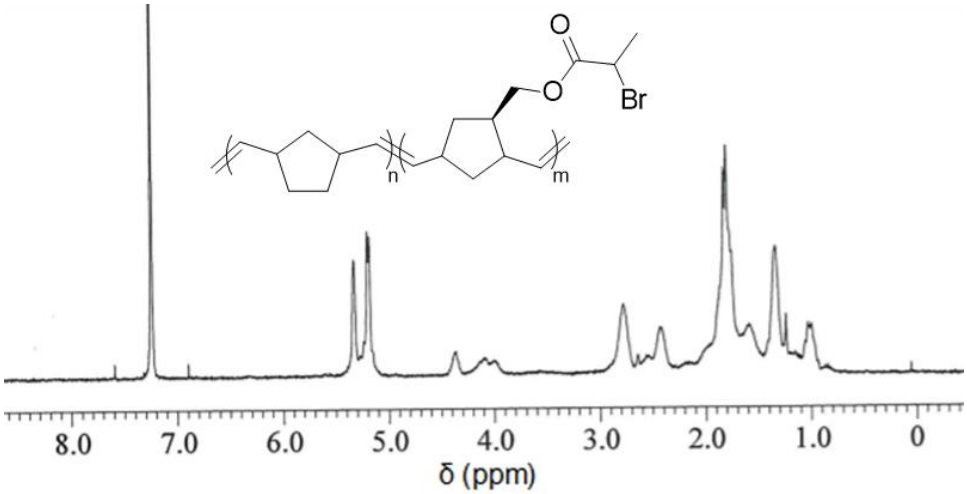

Figure S18. ^{1}H NMR spectrum of block copolymer (**4**) and (**7**) in $CDCl_3$

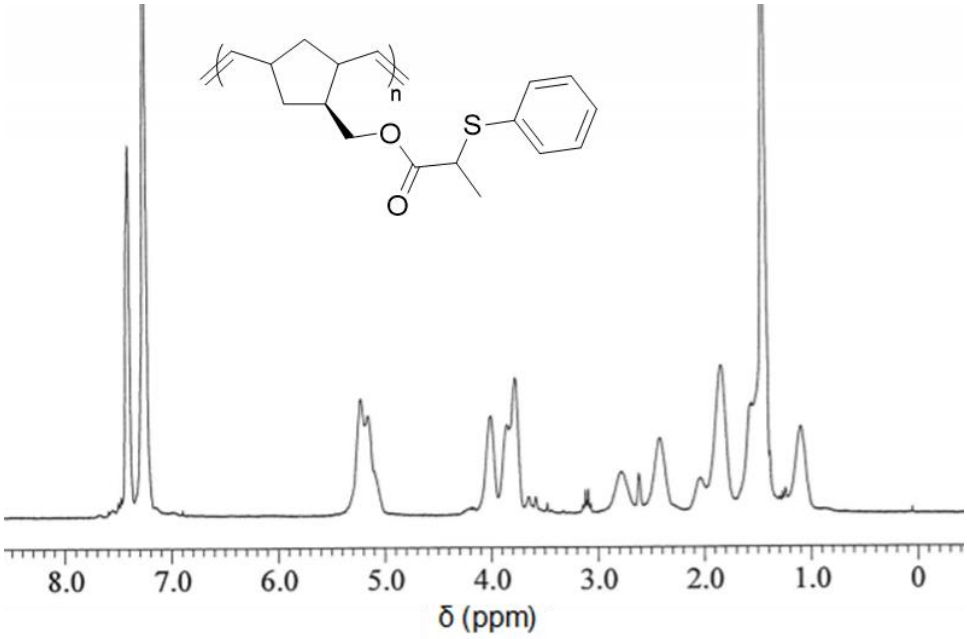

Figure S19. ^{1}H NMR spectrum of polymerized (**7**) followed by click reaction with **15** in $CDCl_3$

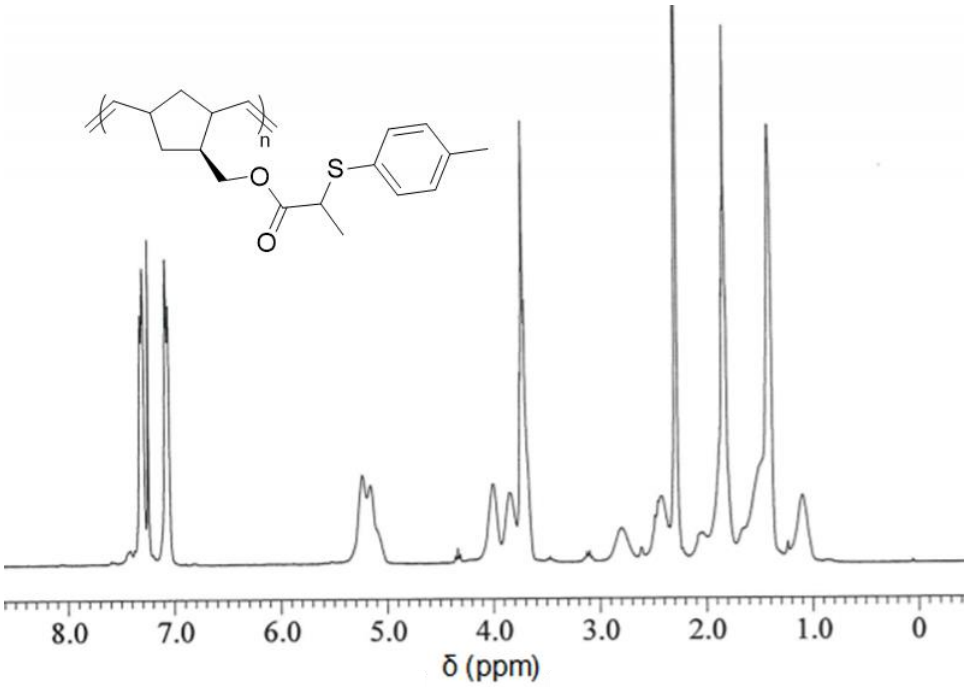

Figure S20. ^{1}H NMR spectrum of polymerized (**7**) followed by click reaction with **16** in $CDCl_3$

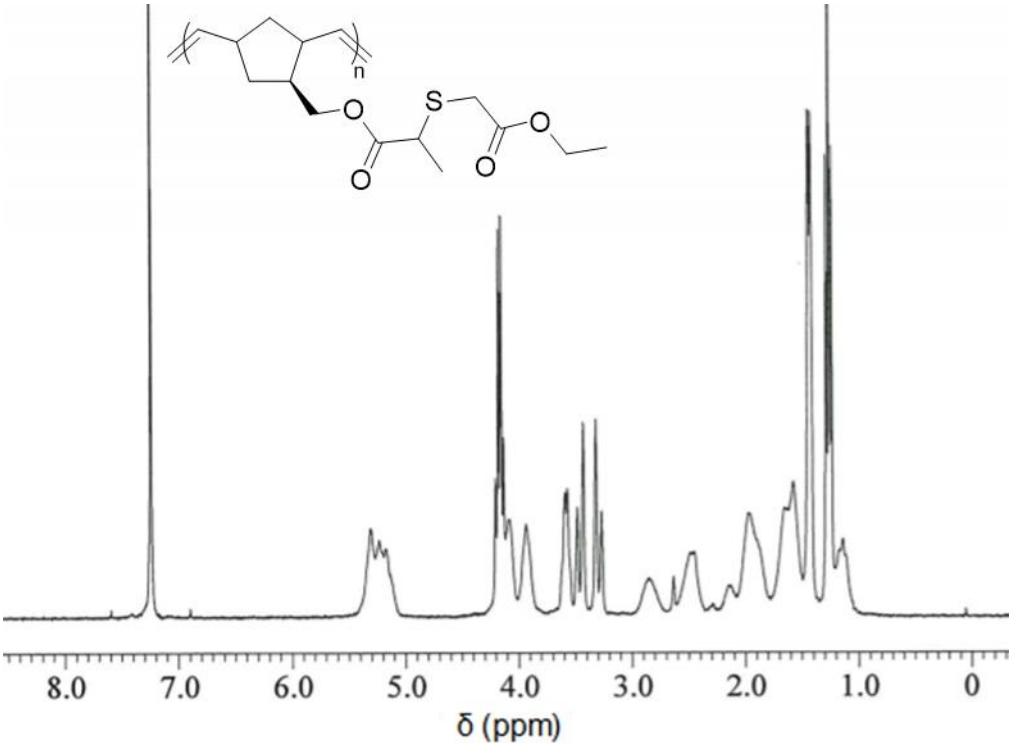

Figure S21. ^{1}H NMR spectrum of polymerized (**7**) followed by click reaction with **17** in $CDCl_3$

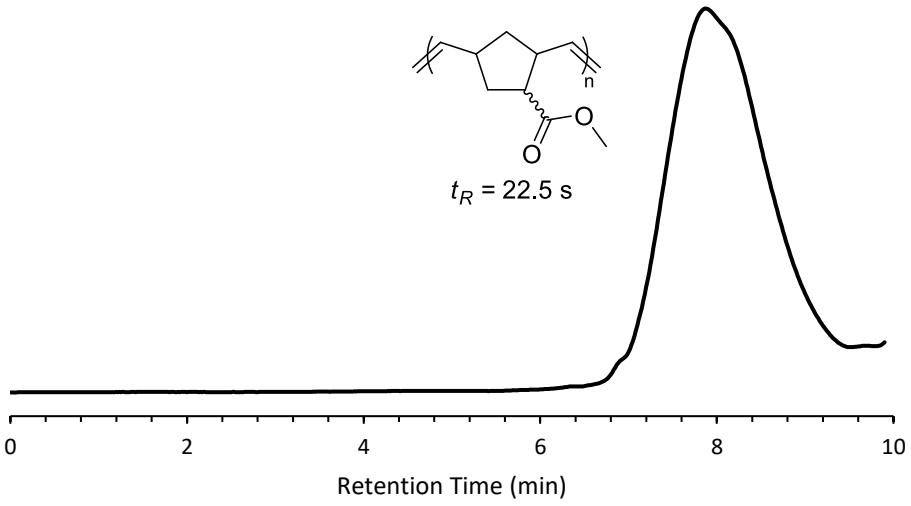

Figure S22. GPC trace of *endo/exo* **5** homopolymerization trace for t_R = 22.5 s

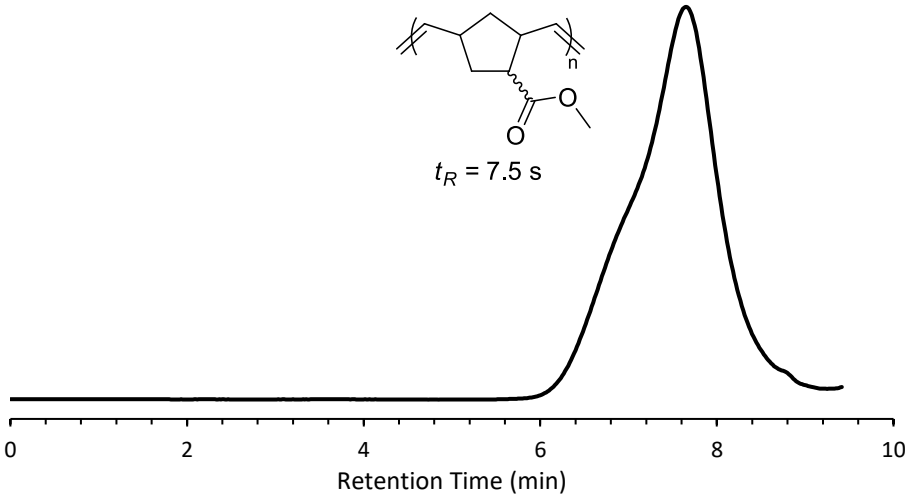

Figure S23. GPC trace of *endo/exo* **5** homopolymerization at t_R = 7.5 s

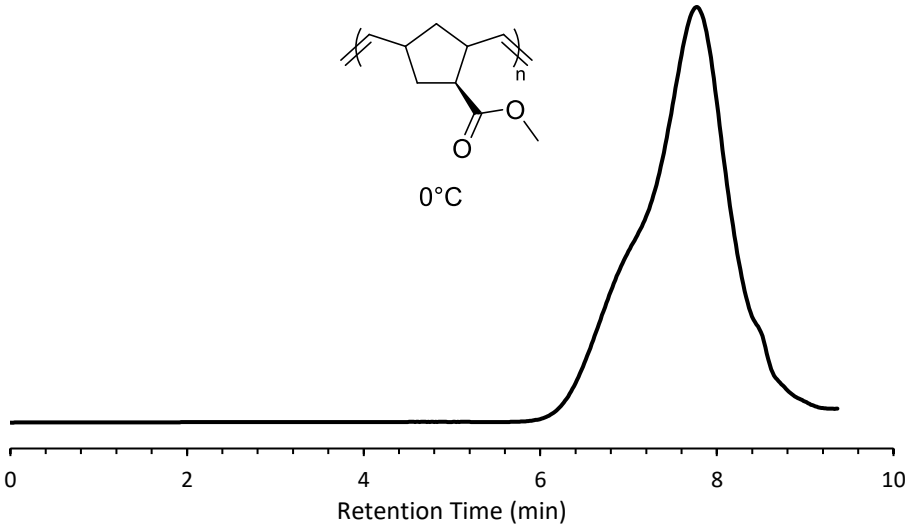

Figure S24. GPC trace of **4** homopolymerization performed at 0°C

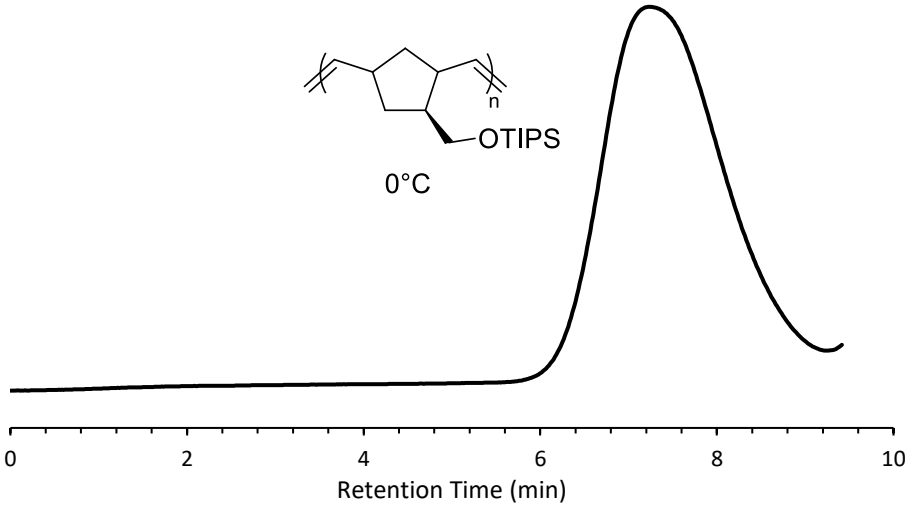

Figure S25. GPC trace of **6** homopolymerization performed at 0°C

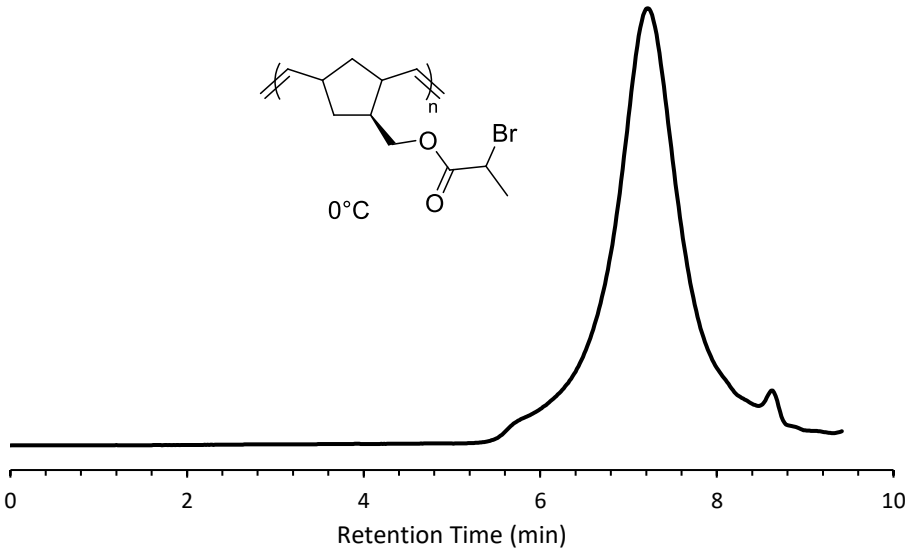

Figure S26. GPC trace of **7** homopolymerization performed at 0°C

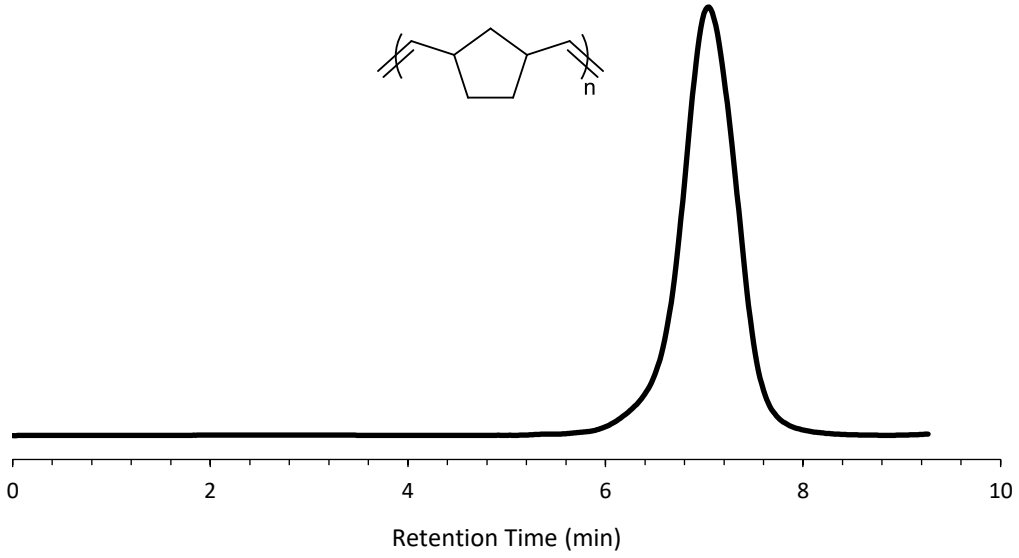

Figure S27. GPC trace of **4** homopolymerization carried out at t_R = 7.5 s

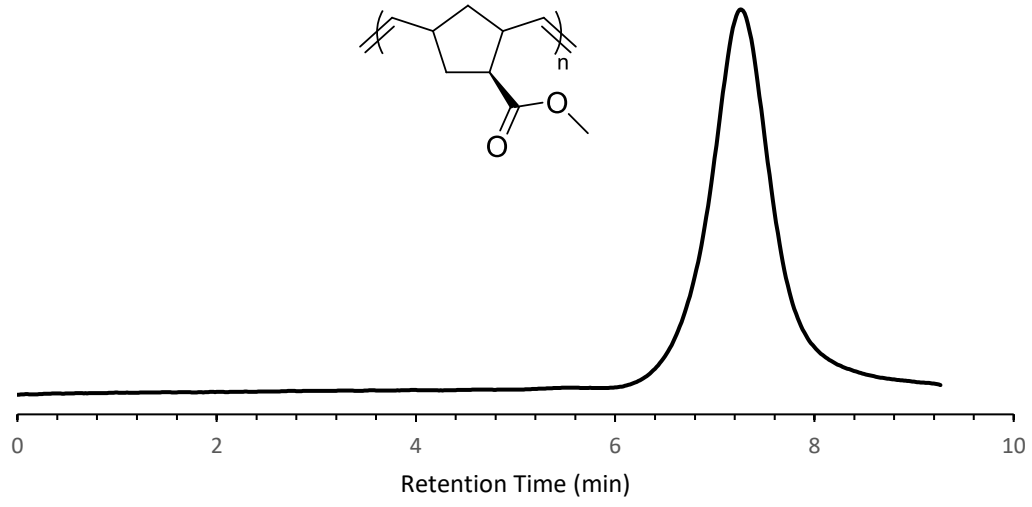

Figure S28. GPC trace of **5** homopolymerization carried out at t_R = 7.5 s

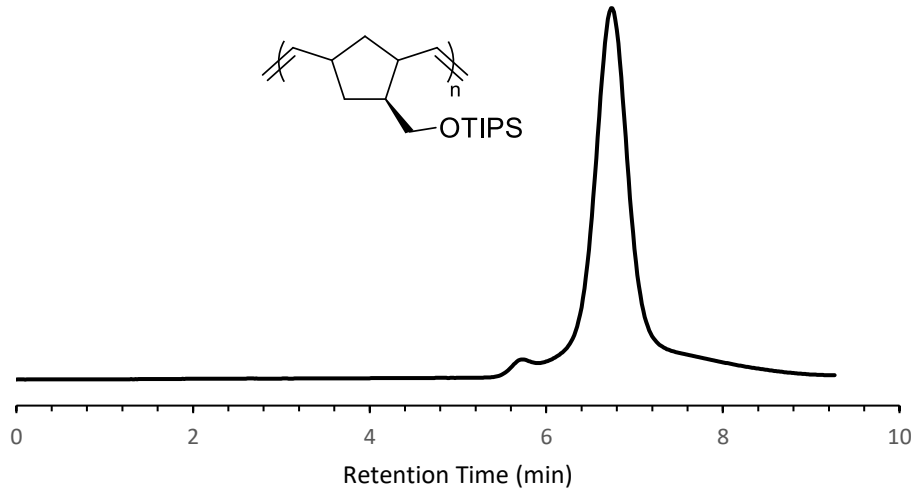

Figure S29. GPC trace of **6** homopolymerization carried out at t_R = 7.5 s

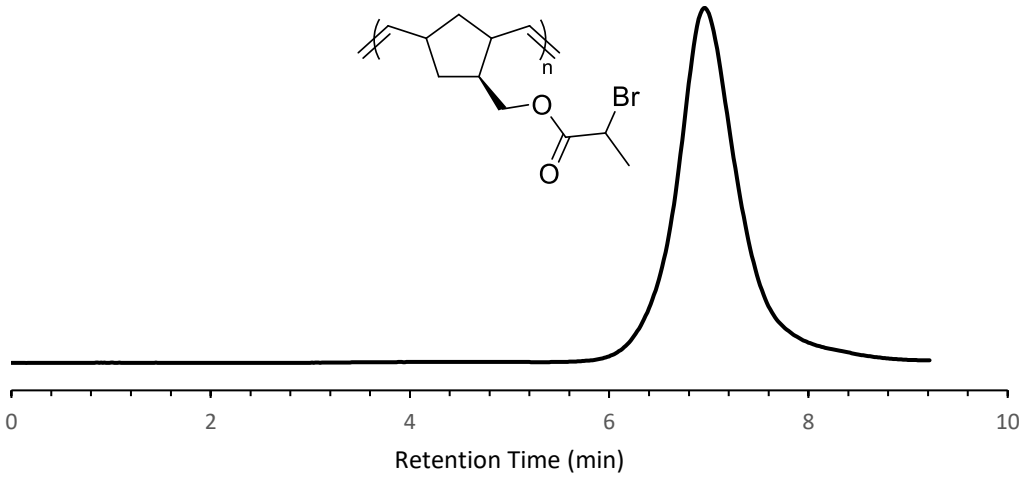

Figure S30. GPC trace of **7** homopolymerization carried out at t_R = 7.5 s

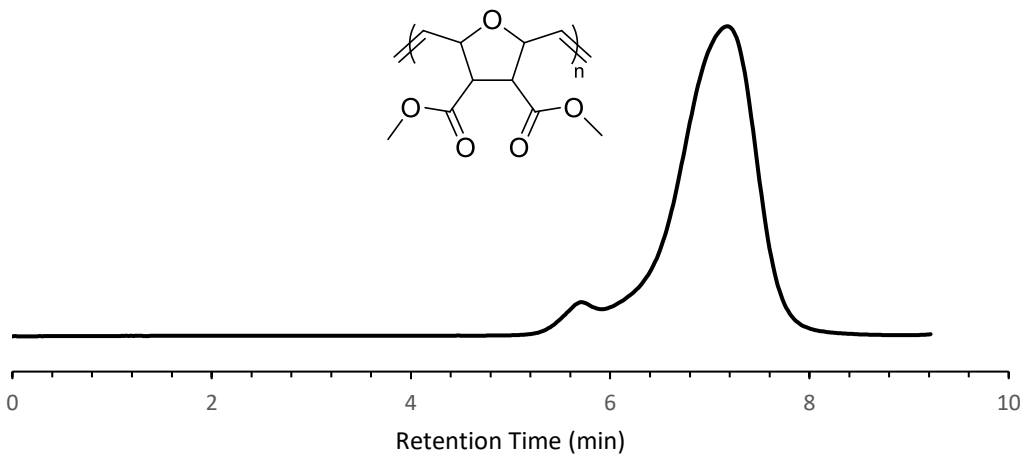

Figure S31. GPC trace of **8** homopolymerization carried out at t_R = 450 s

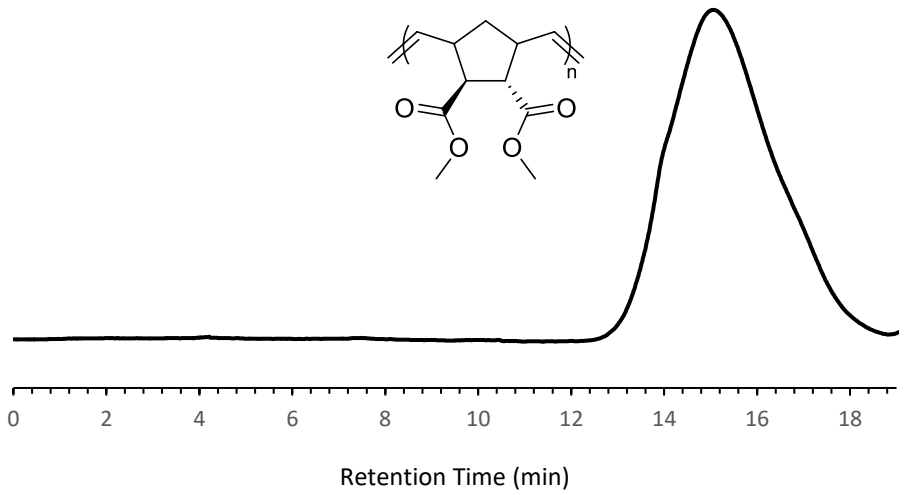

Figure S32. GPC trace of **9** homopolymerization

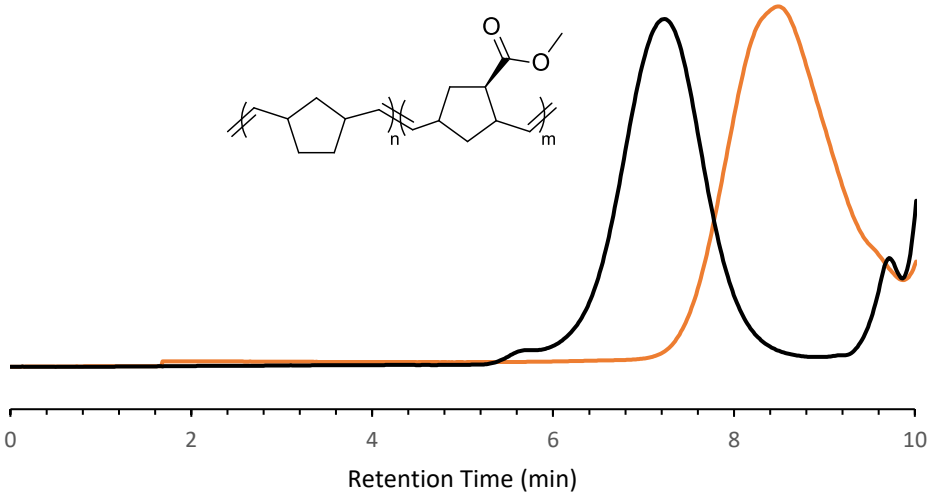

Figure S33. Overlaid GPC traces of first block of **4** (yellow) and generated block copolymer of **4** and **5** (black)

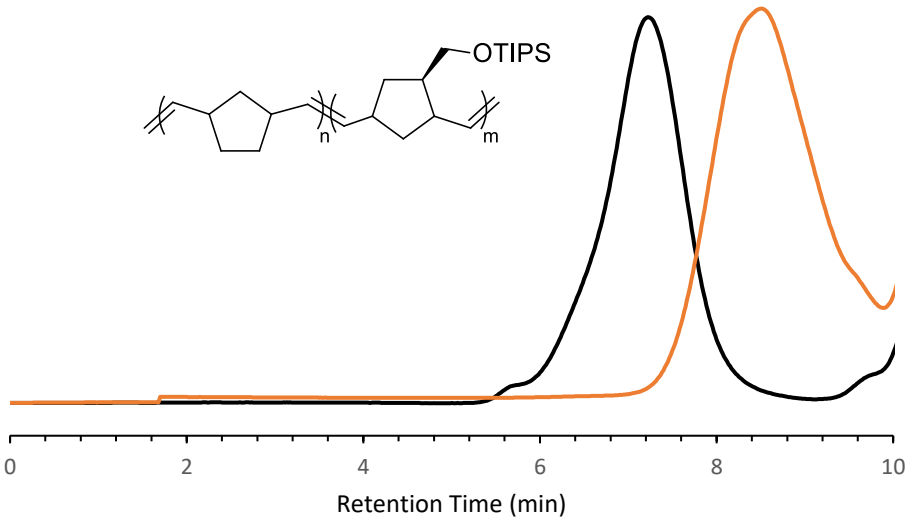

Figure S34. Overlaid GPC traces of first block of **4** (yellow) and generated block copolymer of **4** and **5** (black)

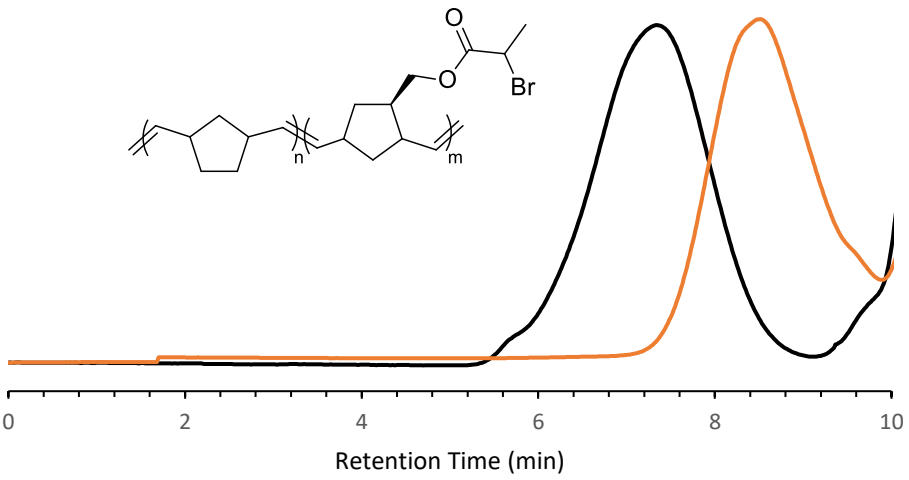

Figure S35. Overlaid GPC traces of first block of **4** (yellow) and generated block copolymer of **4** and **7** (black)

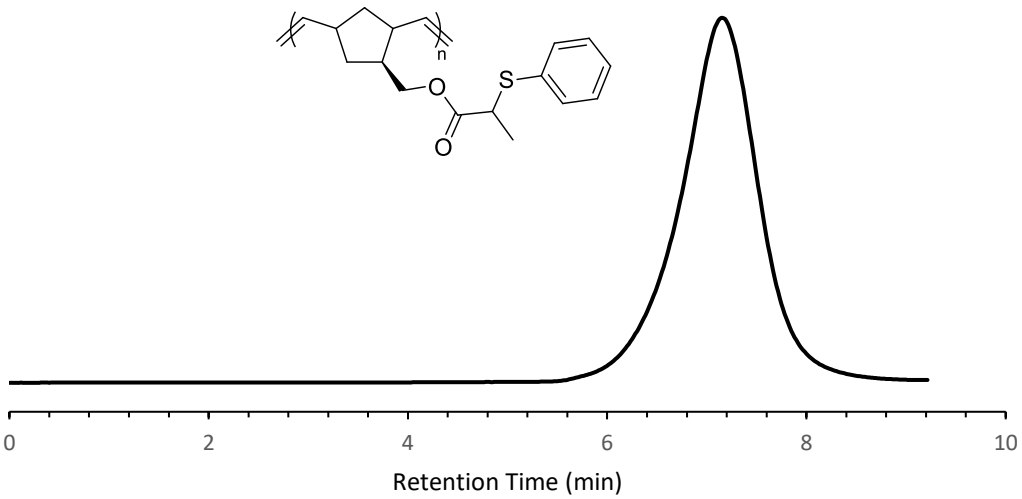

Figure S36. GPC trace of homopolymerization of **7** followed by post polymerization modification utilizing **15**

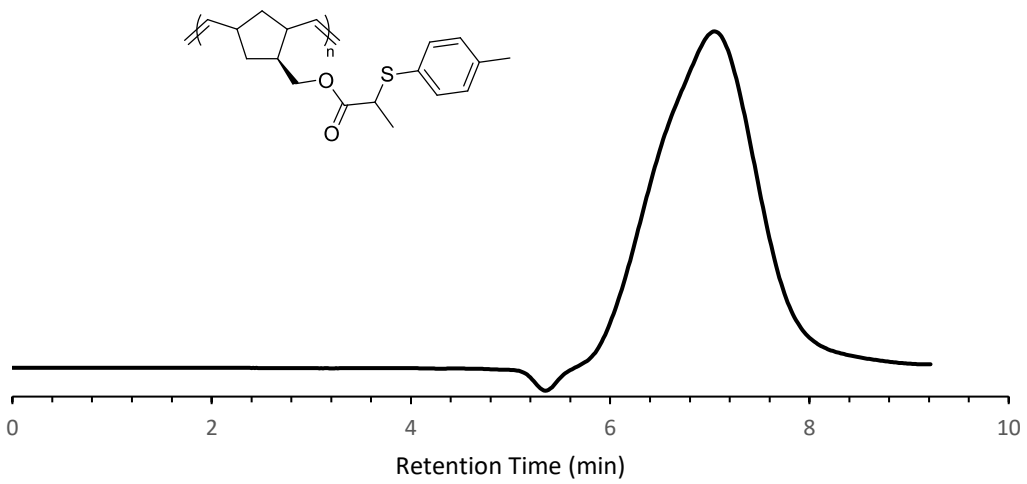

Figure S37. GPC trace of homopolymerization of **7** followed by post polymerization modification utilizing thiol **16**

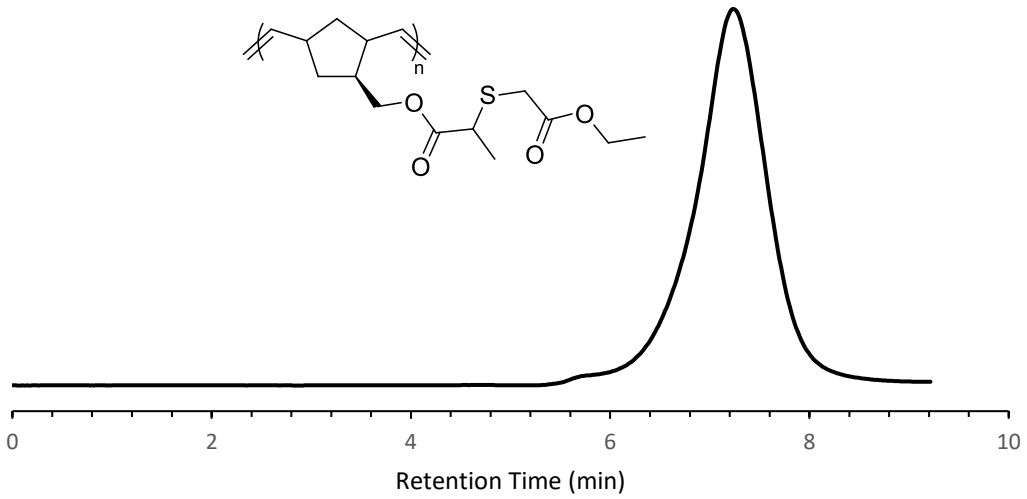

Figure S38. GPC trace of homopolymerization of **7** followed by post polymerization modification utilizing thiol **17**

VITA

SELESHA INDIRA SUBNAIK

EDUCATION

Sam Houston State University 08/2018 to 05/2020

Master of Science in Chemistry

Current GPA: 3.85

Texas A&M University- Corpus Christi 08/2014 to 05/2018

Bachelor of Science in Chemistry—General

Summa Cum Laude Graduation Honors- GPA: 3.96

RELEVANT EXPERIENCE

Sam Houston State University 08/2019 to 05/2020

Graduate Student Researcher under the supervision of Dr. Christopher Hobbs

Graduate Teacher Assistant of Chemistry for the College of Science and Engineering Technology: Organic, General, Inorganic and Environmental Chemistry

Texas A&M University- Corpus Christi 09/2015 to 05/2018

Undergraduate Student Researcher under the supervision of Dr. Fereshteh Billiot:

Characterization of Amino Acid Based Surfactants

Undergraduate Teacher Assistant of Chemistry for the College of Science and Engineering: General Chemistry

PUBLICATION & PRESENTATIONS

Subnaik, S.; Hobbs, C. E. “Flow-Facilitated Ring Opening Metathesis Polymerization (ROMP) Reactions and Post-Polymerization Modification Reactions.” *Polym. Chem.* **2019**, *10*, 4524.

Subnaik, S.; Hobbs, Christopher E. “Performing Ring Opening Meathesis Polymerization (ROMP) reactions under flow conditions.” *257th ACS National Meeting & Exposition*. **2019**. Poster, POLY-0359.

Subnaik, S.; Billiot, F.; Billiot, E.; Morris, K. “Physical properties of undecyl valine surfactant at different pHs.” *255th ACS National Meeting and Exposition*. **2018**. Poster, CHED-404.

Subnaik, S.; Georgiadis, D.; Morris, K.; Blliot, E.; Billiot, F. “Physical properties of mixed CTAB/Octyl-valine based surfactants.” *251st ACS National Meeting and Exposition*. **2016**. Poster, CHED-673.

SKILLS

Wet Laboratory & Safety Training 08/2014 to Present

Through my work in undergraduate and graduate research I have gained experience in performing reactions under air free conditions, practice in organic synthesis, organic product purification methods, and separation techniques.

I have in depth experience with polymer science topics and continuous flow chemistry.

Proficiency in Instrument Operation proficiency References

Nuclear Magnetic Resonance Spectroscopy (NMR), Gel Permeation Chromatography (GPC) and Capillary Electrophoresis (CE)

Specialized Software Experience

Microsoft Office, MathLab and ChemDraw